International Journal of Food Microbiology

Bioactive films with essential oils and machine learning for controlling Aspergillus niger growth and fumonisin B2 production in vitro

--Manuscript Draft--

Manuscript Number:	FOOD-D-25-00299R1 Article available at: https://doi.org/10.1016/j.ijfoodmicro.2025.111251
Article Type:	Full Length Article
Keywords:	bioactive EVOH films; Aspergillus niger; fumonisin B2; essential oils; machine learning; predictive models
Corresponding Author:	Eva María Mateo, Ph.D. University of Valencia Valencia, Valencia SPAIN
First Author:	Fernando Mateo, Ph.D.
Order of Authors:	Fernando Mateo, Ph.D.
	Andrea Tarazona, Ph.D.
	Rafael Gavara, Ph.D.
	Eva María Mateo, Ph.D.
Abstract:	Aspergillus niger is an important species in the fungal community of many foods and is one of the most significant microorganisms used in biotechnology. Some A. niger strains are capable of producing fumonisin B2 (FB2) under certain conditions, but little is known about methods to control them, especially in organic foods. FB2 is a mycotoxin with high toxicity for humans and animals. Effective strategies to control A. niger and FB2 in agricultural commodities are needed. In this study, ethylene-vinyl alcohol (EVOH) copolymer films containing Origanum vulgare (ORE), Cinnamomum zeylanicum (CIN) essential oils (EO) or individual EO components such as carvacrol (CAR) cinnamaldehyde (CINHO), citral (CIT), isoeugenol (IEG) and linalool (LIN) were evaluated as antifungal and anti-fumonisin agents against two isolates of A. niger isolated from organic maize grains grown in Spain. Radial colony growth rate (GR), effective doses to reduce or completely inhibit fungal growth by 50, 90, and 100% (ED50, ED90, and ED100), and FB2 levels were determined in all cultures. Assays were performed under different water activities (aw) (0.95-0.99) and temperatures (20-35 ºC). Machine learning (ML) models to predict GR and FB2 production were developed. Fungal isolate, film type, doses, aw and temperature had significant effects on film efficacy to control A. niger growth and FB2 production. Optimal GR was found at 0.99 aw and 35 °C, and optimal FB2 production occurred at 0.97 aw and 28 ºC. The most effective bioactive film against A. niger and FB2 production was EVOH-CINHO, followed by EVOH-IEG and EVOH-CAR; the worst film was EVOH-LIN. The growth of A. niger was inhibited in the treatments with EVOH-CINHO films at a dose of 250 µg/Petri dish incubated at 20 ºC and 0.95 aw and in the treatments with EVOH films supplemented with IEG, CIT, CAR, or LIN at a dose of 1000 µg/dish. Overall, the XGBoost (extreme gradient boosted tree) and support vector machine (SVM) algorithms generated the most accurate models for predicting GR. The former was also the most effective at predicting FB2 production. This is the first study on the effect of bioactive films supplemented with EO or its main components on A. niger growth and FB2 production. The EVOH films incorporating CINHO, IEG, or CIT examined in this study are strongly recommended as biodegradable component in packaging material to control A. niger and FB2 production in fresh foods, including organic foods.

- Optimal growth of FB2-producing *A. niger* isolates occurred at 37 ºC and 0.99 a_w.
- Optimal FB2 production by *A. niger* isolates occurred at 28 ºC and 0.97 a_w
- EVOH films with cinnamaldehyde were very effective in the control of A. niger and FB2 production.
- Models built with XGBoost were excellent for predicting the growth of A. niger and FB2 production
- ML methods are promising tools for preventing toxigenic fungi and mycotoxins in foods.

Bioactive films with essential oils and machine learning for controlling *Aspergillus niger* growth and fumonisin B_2 production in vitro

Fernando Mateo [a], Andrea Tarazona [b], Rafael Gavara [c], Eva María Mateo [d, *]

[a] Department of Electronic Engineering, ETSE, University of Valencia, Burjassot, Valencia, Spain. Fernando.mateo@uv.es

[b] Department of Microbiology and Ecology, Faculty of Biology, University of Valencia, Burjassot, Valencia, Spain. Andrea.tarazona@uv.es

[c] Packaging Lab, Institute of Agrochemistry and Food Technology, CSIC, Av. Agustín Escardino, No 7, Paterna, Valencia, Spain. Rafael.gavara@iata.csic.es

[d] Department of Microbiology and Ecology, School of Medicine, University of Valencia, Valencia, Spain. Eva.mateo@uv.es

* Correspondence author: Eva María Mateo; email: eva.mateo@uv.es

Abstract

Aspergillus niger is an important species in the fungal community of many foods and is one of the most significant microorganisms used in biotechnology. Some *A. niger* strains are capable of producing fumonisin B2 (FB_2) under certain conditions, but little is known about methods to control them, especially in organic foods. FB_2 is a mycotoxin with high toxicity for humans and animals. Effective strategies to control *A. niger* and FB_2 in agricultural commodities are needed. In this study, ethylene-vinyl alcohol (EVOH) copolymer films containing *Origanum vulgare* (ORE), *Cinnamomum zeylanicum* (CIN) essential oils (EO) or individual EO components such as carvacrol (CAR) cinnamaldehyde (CINHO), citral (CIT), isoeugenol (IEG) and linalool (LIN) were evaluated as antifungal and anti-fumonisin agents against two isolates of *A. niger* isolated from organic maize grains grown in Spain. Radial colony growth rate (GR), effective doses to reduce or completely inhibit fungal growth by 50, 90, and 100% (ED_{50}, ED_{90}, and ED_{100}), and FB_2 levels were determined in all cultures. Assays were performed under different water activities (a_w) (0.95-0.99) and temperatures (20-35 ºC). Machine learning (ML) models to predict GR and FB_2 production were developed. Fungal isolate, film type, doses, a_w and temperature had significant effects on film efficacy to control *A. niger* growth and FB_2 production. Optimal GR was found at 0.99 a_w and 35 °C, and optimal FB_2 production occurred at 0.97 a_w and 28 ºC. The most effective bioactive film against *A. niger* and FB_2 production was EVOH-CINHO, followed by EVOH-IEG and EVOH-CAR; the worst film was EVOH-LIN. *A. niger* growth was inhibited in the treatments with EVOH-CINHO films at a dose of 250 µg/Petri dish incubated at 20 ºC and 0.95 a_w and in the treatments with EVOH films supplemented with IEG, CIT, CAR, or LIN at a dose of 1000 µg/dish. Overall, the XGBoost (extreme gradient boosted tree) and support vector machine (SVM) algorithms generated the most accurate models for predicting GR. The former was also the most effective at predicting FB_2 production. This is the first study on the effect of bioactive films supplemented with EO or its main

components on *A. niger* growth and FB_2 production. The EVOH films incorporating CINHO, IEG, or CIT examined in this study are strongly recommended as biodegradable component in packaging material to control *A. niger* and FB_2 production in fresh foods, including organic foods.

Keywords: bioactive EVOH films, *Aspergillus niger*, fumonisin B_2, essential oils, machine learning, predictive models

1. Introduction

The fumonisins were firstly isolated in 1988 from *Fusarium verticillioides* (previously classified as *F. moniliforme*) cultures and are categorized into four series A, B, C and P. The B-type, comprising fumonisins B_1 (FB_1), B_2 (FB_2), B_3 (FB_3), and B_4 (FB_4), is the most abundant reported in the literature (Braun and Wink, 2018; EFSA, 2018; Yang et al., 2022). Fumonisin exposure has been associated with a variety of adverse outcomes in equines, including leukoencephalomalacia, pulmonary edema in swine, neural tube defects, growth impairment, cardiovascular diseases, and the prevalence of esophageal cancer (Andrade, 2023; Chen et al., 2018; Desjardins, 2006; Kigen et al., 2017, Qu et al., 2022). In the past three decades, most studies on fumonisin production and the corresponding toxigenic genes have centered on two *Fusarium* species, *F. proliferatum* and *F. verticillioides* (Beccari et al., 2020; Junior et al., 2018; Rheeder et al., 2002; Stępień et al., 2011; Tarazona et al., 2021). These species have been recognized as the largest fumonisin producers, mainly in cereals and cereal-based foods, with maize and maize-based products being the food category with the highest expected incidence (Farhadi et al., 2021; Lee and Ryu, 2017; Marasas et al., 1988; Tarazona et al., 2020). Type B fumonisin production at low levels by other *Fusarium* spp., including *F. dlaminii*, *F. napiforme*, *F. nygamai* and *F. oxysporum,* has also been documented (Nelson et al., 1992).

Therefore, fumonisins, which were considered to be produced exclusively by a limited number of *Fusarium* species, have emerged as economically important mycotoxins. The correlation between certain *Fusarium* spp. and fumonisins in food was altered when Frisvad et al. (2007) and Noonim et al. (2009) found that certain industrially and freshly strains of *A. niger* from coffee beans produced FB_2. These findings highlighted the potential toxicological risks associated with foods colonized by this species. *A. niger* can produce FB_2 at levels comparable to those produced by *F. verticillioides* (Frisvad et al., 2007; Han et al., 2017) and FB_4 and FB_6 (Mansson et al.,

2009; Mogensen et al., 2010a; Noonim et al., 2009). However, FB_2 is the predominant fumonisin produced by *A. niger*, particularly when cultivated on agar substrates with high amounts of sugar, glycerol or NaCl (Frisvad et al., 2007; Mogensen et al., 2009; Varga et al., 2010).

These findings raise the possibility of fumonisin contamination in various agricultural commodities, including maize (Tarazona et al., 2020), cocoa (Copetti et al., 2014), coffee beans (Noonim et al., 2009), animal feed (Amézqueta et al., 2012) and, notably, grapes. *A. niger* is the most frequent contaminant in grapes. The presence of this species has been documented in various *Vitis* spp. worldwide and it has been linked, in conjunction with *A. carbonarius,* to the occurrence of ochratoxin A (OTA) in grape, grape must, and wine (Chiotta et al., 2013; Ferranti et al., 2018; García-Cela et al., 2015; Gil-Serna et al., 2018; Mateo et al., 2007; Pantelides et al., 2017; Qi et al., 2016). However, less attention has been paid to FB_2 in grapes and derivatives (Knudsen et al., 2010; Logrieco et al., 2009, 2010; Mogensen et al., 2010b; Perrone et al., 2013; Varga et al., 2010). Although FB_2 and OTA have been classified as possible human carcinogens in group 2B (IARC, 1993), only OTA is regulated in wine, grape juice, and dried vine fruits in the current EU legislation. However, the sum of FB_1 and FB_2 levels in maize and maize-products is subject to regulation, with maximum levels ranging from 200 to 4,000 µg/kg (Commission Regulation (EU) 2023/915).

Although, for a long time, chemical antifungal agents are being used to control fungal growth and mycotoxin production in food, the application of these chemicals to control fungi and mycotoxins increases the risk of toxic residues in food and feed, induces fungal resistance, and their use in organic foods is not permitted.

In the last years there has been a growing interest in the preparation of innovative materials for smart food packaging including self-healing materials, which can repair damaged packaging areas, restore the original properties and prevent the decline of food quality (Wang et al., 2024a) or nanomaterials, such as zein self-assembled nanoparticles

using a variety of treatment to exploit its potential advantages as carrier for bioactive substances (Feng et al., 2025).

Presently, there is a mounting interest in the development of innovative strategies to control fungal growth and mycotoxin production in foods, especially in organic foods. Among these strategies, active packaging systems have attracted significant attention. Active packaging offers the possibility of containing active molecules/ingredients in packages that interact with the food environment or the food itself, thus reducing the amount of food additives in food products, maintaining unaltered the quality, safety and organoleptic characteristics of food products and extending their shelf-life (Luzi et al., 2020; Muriel-Galet et al., 2015). Ethylene–vinyl alcohol (EVOH) copolymers are flexible, glossy, have high transparency, high resistance to hydrocarbons, oils and organic solvents, high flexibility, excellent flex-crack resistance, and excellent gas barrier properties against O_2, N_2, and CO_2. These properties make these systems particularly suitable for food packaging applications (Muriel-Galet et al., 2014, 2015).

Among the active ingredients that can be incorporated into food-packaging system, essential oils (EOs) must be highlighted. Plant-derived EOs and their individual components (EOCs) are natural substances categorized as GRAS (Generally Recognized as Safe) by the US Food and Drug Administration. They have been the focus of extensive research not only because they are natural products but also because they have demonstrated benefits in human health and food preservation, such as antitumor, analgesic, antidiabetic, anti-inflammatory, insecticidal, antioxidant, and antimicrobial properties (Periasamy et al., 2016; Yen et al., 2015). Moreover, EOs show a low risk of resistance development in pathogenic and spoilage microorganisms.

Research on the possible applications of bioactive films containing EOs/EOCs in the control of toxigenic fungi and mycotoxins in food is scarce (Mateo et al., 2017, 2021; Sun et al., 2020; Tarazona et al., 2021). There are no previous studies on the effect of bioactive EVOH films in preventing or delaying *A. niger* growth and FB_2 production. Fungal growth and fumonisin production also depend on various factors, mainly,

temperature and water activity (a_w) (Frisvad et al., 2007; Mogensen et al., 2009). Therefore, the influence of temperature and a_w on the efficiency of these bioactive films should be investigated. These are complex processes, and predicting them with the help of machine learning (ML) methods can be very useful.

The application of ML methods in the microbiology field, including the prediction of fungal growth and mycotoxin production, is scarce, although several studies have shown its great potential in this field (Camardo Leggieri et al., 2021, Mateo et al., 2017, 2021; Qu et al., 2019; Shelke et al., 2023; Smith et al., 2020). ML algorithms such as extreme gradient boosting trees (XGBoost), random forest (RF), multi-layer perceptron neural network (MLP) or support vector machine (SVM) could be excellent tools in the management of fungi and mycotoxins in food. XGBoost is an ensemble learning method based on decision tree boosting. It uses gradient boosting to iteratively improve the model by focusing on the residual errors of previous trees, making it highly effective in handling complex, nonlinear relationships in data and is popular due to its scalability and performance in classification/regression tasks (Chen and Guestrin, 2016). RF is an ensemble learning method that builds multiple decision trees and combines their predictions. Each tree is trained on a bootstrap sample of the data, and the decision process considers a random subset of features at each split. This diversity among the trees helps improve the robustness of the model and prevent overfitting (Breiman, 2001; Liaw and Wiener, 2002). SVM is a supervised learning algorithm used for classification and regression. It works by finding a hyperplane that best separates the data into different classes, or for regression, it tries to fit the data within a margin while minimizing errors (Cortes and Vapnik, 1995). MLP is a type of artificial neural network (ANN) consisting of multiple layers of nodes. It uses backpropagation for training, and adjust weights through the network to minimize prediction errors. It can model complex relationships between input and target variables (Rumelhart et al., 1986).

The objectives of the present work were *i*) to assess the efficacy of EVOH films incorporating oregano or cinnamon bark EO or the EOCs carvacrol, cinnamaldehyde,

160 citral, isoeugenol and linalool in controlling *A. niger* growth and FB_2 production under
161 different temperature and a_w regimes and *ii*) to evaluate the potential of various ML
162 methods to predict *A. niger* GR and FB_2 production under the assayed conditions.

163 ## 2. Materials and methods

164 *2.1. Film Preparation*

165 Ethylene vinyl alcohol copolymer with 29% ethylene molar content (EVOH-29)
166 was kindly supplied by The Nippon Synthetic Chemical Industry Co., Ltd. (Osaka,
167 Japan). Oregano EO (*Origanum vulgare*) (ORE) containing 86% carvacrol and cinnamon
168 bark (*Cinnamomum zeylanicum*) (CIN) containing 66.5% trans-cinnamaldehyde were
169 purchased from Jarpil (Almería, Spain). Carvacrol (CAR), trans-cinnamaldehyde
170 (CINHO), citral (CIT), isoeugenol (IEG) and linalool (LIN) were supplied by Sigma-Aldrich
171 (Barcelona, Spain). The preparation of the EVOH films and the final content of the EO
172 or EOC in the bioactive films was carried out as previously described (Cerisuelo et al.,
173 2012; Mateo et al., 2017; Tarazona et al., 2018, 2021).

174 The EVOH films containing the EOs/EOC were obtained by dissolving 13 g of
175 EVOH-29 pellets in 100 ml of 1–propanol/pure water 1:1 (v/v) by heating at 75 °C under
176 reflux. When the copolymer was dissolved, the EO or EOC was added (1, 5 and 10%
177 w/w dry polymer). The mixture was stirred at 40 °C for 30 min and spread on a Teflon-
178 coated glass plate by using a 200-µm spiral bar coater providing films with a thickness
179 of 13 ± 2 µm. EVOH films without active substances were used as controls.

180 The final contents of the EOs/EOCs in the films were determined as described in
181 detail in Cerisuelo et al. (2012) by thermal desorption-gas chromatography, using an 890
182 thermal tube desorber connected to a HP 5890 Series II Plus gas chromatograph (Agilent
183 Tech., Barcelona, Spain) equipped with a flame ionization detector and an Agilent HP-1
184 column of 30 m length, 0.53 mm i.d and 2.65 µm film thickness. A portion of the film
185 (about 20 mg) was placed in a desorption cell and heated at 210 °C for 7 min. A stream
186 of He carried the desorbed compounds to the GC through a transfer line heated at 230

°C. At the end of the process the film sample was weighed. Additional desorption processes proved that all the volatile additives were desorbed in the first process. The GC response was calibrated by measuring samples containing known amounts of CINHO, CAR, LIN, IEG and CIT. The films were labeled as EVOH-ORE, EVOH-CIN, EVOH-CAR, EVOH-CINHO, EVOH-CIT, EVOH-IEG, and EVOH-LIN. The film grammage was 1.79 ± 0.02 mg film/cm^2. The additive content is expressed as weight percentage of the compound over dry polymer weight. The final EO/EOC contents in the films were 0.37 ± 0.06%, 1.85 ± 0.25% and 3.7 ± 0.5%, w/w of dry polymer, for the films prepared at 1, 5 and 10% w/w respectively. Loss of active compounds are due to evaporation during the preparation process. The films were stored in chambers at room temperature in the presence of a dehydrating agent.

2.2. Standards and reagents

Corn steep liquor and a standard of fumonisin B_2 was supplied by Sigma–Aldrich (Alcobendas, Spain). Formic acid and ammonium formate were purchased from Panreac (Castellar del Valles, Spain). Methanol (LC grade) and 1-propanol were purchased from J.T. Baker (Deventer, the Netherlands). White rice was from local sources; it was previously analyzed and found to have undetectable FB_2 level before its use. Pure water was delivered from a Milli-Q system (Millipore, Billerica, MA, USA).

2.3. Fungal isolates and inoculum preparation

Two FB_2-producing isolates of *A. niger* (designated as An2 and An14) from ecological maize grains grown in Spain were previously selected and, subsequently, used in this study. The *A. niger* isolation was conducted from maize samples obtained in Spain (Tarazona et al., 2020). Maize samples were ground, and serial decimal dilutions were prepared in sterile saline (9 g NaCl/l pure water). From each dilution, a 100-µl aliquot was dispensed onto the surface of Potato Dextrose Agar (PDA) Petri dishes. The inoculated plates were incubated at 28 °C for five days. The *A. niger* aggregate isolates were identified on the basis of their colony appearance and their morphological

214 characteristics under microscopic visualization, including the presence of biseriate
215 conidiophores, which produce small and non-ornamented conidia (Samson et al., 2007).
216 The isolates were stored as spore suspensions in 15% glycerol at -80 °C, and
217 subsequently cultured on PDA when required. The *A. niger* isolates were identified using
218 species-specific PCR assays (Gil-Serna et al., 2019). The phenotypic characterization of
219 the isolates as FB_2 producers was performed by UPLC-MS/MS (Section 2.6).

220 Both isolates are stored in the Mycology and Mycotoxin Group Culture Collection
221 (Valencia University, Spain). The isolates were grown on PDA (Samson et al., 2004) and
222 incubated at 25 °C for seven days in a dark environment. These fresh cultures were
223 subsequently utilized to prepare inocula for further experiments. Prior to each
224 experiment, a suspension containing 1.0×10^6 conidia/ml was prepared in sterile pure
225 water containing Tween 80 (0.005%) using a Thoma cell counting chamber.

226 *2.4. Preparation of fungal cultures with different EVOH films and* a_w *levels*

227 The medium used for *A. niger* growth and FB_2 production was Rice Corn Steep
228 (RC) Agar It was prepared in flasks containing pure water, 5% rice powder, 4% corn
229 steep liquor and 2% agar (Bullerman, 1974). The a_w was adjusted in all flasks to 0.99 ±
230 0.002, 0.97 ± 0.001 and 0.95 ± 0.003 by adding different concentrations of NaCl (2.0-
231 7.5%) using a previously determined adsorption curve for RC agar. Culture media were
232 placed into Erlenmeyer flasks and autoclaved for 20 min at 121 °C. After autoclaving,
233 the a_w-values of the media were checked. The a_w-values were measured with a Novasina
234 RTD 502 instrument (Novasina GmbH, Pfäffikon, Switzerland) using controls of known
235 a_w supplied by the manufacturer. Twenty ml of medium was placed into each of 9-cm
236 diameter Petri dishes. Circular pieces of each bioactive EVOH film were prepared to
237 achieve final average doses of 250, 1000, 1500, and 4000 µg of each EO or EOC per
238 piece. To attain these doses, the circle diameters and the concentrations of EO/EOC in
239 the films, considering the average film grammage, were as follows: 7.0 cm of the film
240 with 0.37% (250 µg), 6.2 cm of the film with 1.85% (1000 µg), 7.6 cm of the film with

241 1.85% (1500 µg), and 8.8 cm of the film with 3.7% (4000 µg) (see Section 2.1). The
242 pieces were affixed on the base of the Petri dish lid using double-sided adhesive
243 cellophane. Subsequently, 5 µl of a spore suspension of *A. niger* containing 1.0×10^6
244 spores/ml was inoculated by single central point, immediately capped and sealed with
245 Parafilm. The Petri dishes undergoing the same treatment were enclosed in plastic
246 containers together with beakers of a glycerol–water solution matching the same a_w as
247 the treatments. Treatment and control cultures were incubated at 20, 28 and 35 ºC in the
248 dark for 12 days. Experiments were performed in triplicate and repeated twice on two
249 non-consecutive days.

250 *2.5. Effect of treatments on fungal growth*

251 Growth in treatment and control cultures was monitored daily according to
252 Tarazona et al. (2021). Colony radius was calculated as the sum of two perpendicular
253 diameters divided by four. Radial GR (mm/day) was calculated as the slope of the line
254 obtained by linear regression of mean colony radius *versus* time (only the linear part of
255 this graph was used). The doses of active compounds in the EVOH film/plate required
256 for 50%, 90% and 100% growth inhibition (ED_{50}, ED_{90} and ED_{100}) were estimated, where
257 possible, from the plots of GR *versus* doses of active ingredient in the films.

258 *2.6. Effect of treatments on mycotoxin production*

259 2.6.1. Mycotoxin determination in RC agar with different a_w

260 At the end of the incubation period, regardless of fungal colony size, the total
261 culture (substrate plus fungal biomass) in controls and treatments was removed from
262 Petri dishes, homogenized using a stomacher and analyzed for FB_2 production following
263 the methodology described by Frisvad et al. (2007) with some modifications. One gram
264 of the homogenate was placed in a 4-ml glass vial and mixed with 2.0 ml of a solution of
265 methanol:water (70:30, v/v). FB_2 was extracted by ultrasonication for 50 min. The extract
266 was filtered through a 0.45-µm Nylon syringe filter into another vial and used for analysis
267 by UPLC-MS/MS as described below.

268 2.6.2. UPLC–MS/MS conditions

269 The UPLC–MS/MS system used, and the separation and MS/MS conditions were
270 previously detailed in Tarazona et al. (2021). The mobile phase was a time-programmed
271 combination of water containing ammonium formate (0.15 mmol/L) and formic acid
272 (0.1%) (solvent A) and methanol (solvent B) at a flow-rate of 0.35 ml/min. For FB_2
273 determination two product ions were monitored in multiple reaction monitoring
274 chromatograms. They were the q1 ion (quantifier) and the q2 ion (qualifier)
275 corresponding to m/z transitions 706 to 336.5 and 706 to 354.3, respectively. The q1 ion
276 (the most abundant) is the result of the loss of two tricarboxylic acid groups plus one
277 water molecule from the mother ion $[M+H]^+$ (Logrieco et al., 2009). The q2 ion results
278 from the loss of two tricarboxylic acid groups. The cone voltage was 50 V and the collision
279 energy was 40 eV. Mycotoxin identification was based on the retention time (10.0 ± 0.2
280 min) of the peaks. The q1/q2 ratio (< 20% variation) was used as an additional criterion
281 for identification. Data acquisition/processing was performed using Masslynx 4.1™
282 software (Waters).

283 2.6.3. Calibration and validation

284 Calibration was performed by injecting standard solutions of FB_2 in
285 methanol:water (70:30, v/v) at variable concentrations (1.0 to 5000 ng/ml) in triplicate
286 into the UPLC–ESI(+)–MS/MS system. The calibration line was obtained by weighted
287 linear regression (weighting factor = 1/x) of q1 ion peak areas *versus* concentration. FB_2
288 recoveries were calculated by spiking 1 g of a RC agar culture of a non-producing *A.*
289 *niger* isolate grown during twelve days and homogenized as the cultures of producing
290 isolates with standard solutions of FB_2 at various concentrations (40, 200, 1000, 2500
291 and 5000 ng/g) after overnight incubation at room temperature. They were then
292 processed as described for cultures and injected into the UPLC–ESI(+)–MS/MS system.

293 *2.7. Data analysis*

294 2.7.1. Analysis of variance

295 Data were analyzed by univariate analysis of variance using IBM SPSS ver. 29.0
296 statistical package (IBM, Armonk, NY, USA). The *post-hoc* Tukey's HSD test (α = 0.05)
297 was used to detect homogeneous groups when significant differences between variables
298 were found. To reduce data spread FB_2 concentration values were transformed as the
299 decimal logarithm of x+1 (*log*(x+1)), where x was the FB_2 level. For statistical analysis,
300 FB_2 concentrations < LOQ were considered as zero.

301 2.7.2. ML model development

302 The ML algorithms evaluated for prediction of fungal GR and FB_2 production by
303 the two *A. niger* isolates were XGBoost, RF, MLP and SVM. The software was performed
304 using Phyton version 3.8, with ML models implemented using the *scikit-learn* library
305 version 1.5.1, which provides robust implementations of the aforementioned algorithms,
306 along with utilities for parameter tuning and cross-validation (Pedregosa et al., 2011).
307 The two isolates were treated in two ways: together and separately. The input
308 variables were "isolate", "temperature", "a_w", "bioactive EVOH film" and "dose". The
309 output variables were the "mean GR" and the "mean FB_2 concentration". For the FB_2
310 outputs, the logarithm of the mean FB_2 concentration plus 1 was also calculated to
311 reduce data scatter and to avoid problems with zero values. The preprocessing steps of
312 the variables involved several key transformations to prepare the datasets for ML model
313 training. The categorical variables "isolate" and "bioactive EVOH film" were encoded
314 using One-Hot Encoding, which transformed them into binary columns to make them
315 suitable for analysis. Numerical features "dose", "temperature", and "a_w" were
316 standardized so that all features had a mean of 0 and a standard deviation of 1. After
317 encoding and scaling, the processed features were concatenated into a single dataframe
318 that was used as input to the ML models. This preprocessing process ensured the
319 dataset was optimally formatted for effective model training and prediction. For each
320 experiment, the data was divided into training (80%) and test (20%) sets. The first was

used to build and validate the models. The test set was separated and used to evaluate the performance of the models on independent external data not previously used to build the models. To optimize model performance, a grid search was performed over the hyperparameters of each algorithm. Grid search explores a range of parameter values to identify the optimal combination for each model. Model performance was assessed using five-fold cross-validation, where the data is divided into five subsets, and the model is trained and validated on different folds to ensure robust performance and prevent overfitting. The performance evaluation of the ML models was based on the mean square error (MSE). The R^2 (coefficient of determination) values of the regression line of predicted *versus* real output values were determined for each model and averaged over all five-fold cross-validation. To get the best performance, the goal is to achieve the lowest MSE when applied to the test set, and to obtain a high R^2 value (close to 1.0). Cross-validation and grid search were implemented using the GridSearchCV function from *scikit-learn*, which allows systematic evaluation of multiple hyperparameter combinations and the selection of the best model based on cross-validation results. Table 1 lists the hyperparameters and their values for the algorithms used in this study. These values were tuned during the computational process to find the optimal architectures.

3. Results

3.1. Antifungal activity of bioactive EVOH films

Usually circular, visible and measurable colonies were observed on the fungal cultures when growth occurred. In this case, the delay was 2–3 days depending on the culture conditions. Fig. 1 shows the results for GR on control and treatments of An2 and An14 isolates using EVOH films supplemented with ORE and CIN. Fig. 2 shows the results for GR on control and treatments of both isolates using EVOH films supplemented with CAR, CINHO, CIT, IEG and LIN. The GR of both isolates was in the order: 35 ºC > 28 ºC > 20 ºC and 0.99 a_w > 0.97 a_w > 0.95 a_w. Isolate An2 grew faster than isolate An14

348 under identical conditions. For a given treatment (film type and dose) GR increased with
349 increasing a_w and temperature. For a given film type, temperature and a_w, GR decreased
350 with increasing dose regardless of the isolate. Statistical analysis of the data for both
351 isolates showed that the GR of the control groups, considering all the values of the
352 factors involved, is significantly different from the treatments (*post hoc* HSD Tukey's test,
353 $\alpha = 0.05$). No treatment stimulated fungal growth compared to the corresponding
354 controls.

355 EVOH-CINHO followed by EVOH-IEG were the most effective films for
356 reducing/inhibiting the growth of both isolates of *A. niger*. At CINHO doses of 1500
357 µg/plate and IEG doses of 4000 µg/dish, no growth was observed at any temperature/a_w
358 combination (Fig. 2). For each isolate, film type, dose, temperature and a_w and their
359 interactions significantly affected GR. The homogeneous groups found by the Tukey's
360 test ($\alpha = 0.05$) appear in Table 2. The efficacy of the films against the isolate An14 of *A.*
361 *niger* followed the order: EVOH-CINHO > EVOH-IEG > EVOH-CIT > EVOH-CAR >
362 EVOH-ORE > EVOH-CIN > EVOH-LIN (seven homogeneous groups). For isolate An2
363 the order of efficacy of the films was quite similar although five homogeneous groups
364 were found: EVOH-CINHO > EVOH-IEG > EVOH-CIT > EVOH-CAR ≈ EVOH-ORE >
365 EVOH-CIN ≈ EVOH-LIN. For both isolates, the four doses of EO/EOC tested were
366 grouped into four homogeneous groups and their efficacy varied in the order 4000 >
367 1500 > 1000 > 250 µg/dish, as expected.

368 The ED_{50}, ED_{90} and ED_{100} of bioactive films were estimated from plots of GR
369 *versus* EO/EOC dose in the film. The results of the mean values for EVOH-ORE and
370 EVOH-CIN films are shown in Table 3 and for EVOH-CAR, EVOH-CINHO, EVOH-CIT,
371 EVOH-IEG, and EVOH-LIN films in Table 4. Effective EO or EOC doses generally
372 increased with increasing temperature and a_w, regardless of film type. The lower EDs for
373 both isolates were attained by EVOH-CINHO, followed by EVOH-IEG and EVOH-CIT,
374 which are very close, in agreement with the results of the statistical treatment of the GR
375 data mentioned above. A dose of 220 µg CINHO/dish in EVOH films can reduce the

376 growth of both isolates by 50% with respect to the controls at all temperatures and a_w
377 tested, while a dose of 1500 µg CINHO/dish completely inhibited the growth of both
378 isolates at all temperatures/a_w tested (Table 4). The highest EDs were recorded for the
379 EVOH-CIN and EVOH-LIN treatments. For EVOH-LIN the only ED_{100} < 4000 µg/dish was
380 910 µg/dish achieved at 20 ºC/0.95 a_w.

381 *3.3. Validation of the UPLC-ESI-MS/MS method for FB_2 determination*

382 FB_2 recovery in spiked samples at five levels (40, 200, 1000, 2500 and 5000 ng/g)
383 averaged 79% (range 68.3%–92.7%) and the mean relative standard deviation of
384 recoveries was 8.9% (range 11.4–6.3%). The limit of detection (LOD) was estimated as
385 LOD = 3.3×$s_{y/x}$/b, where $s_{y/x}$ is the residual standard deviation of the regression and *b is*
386 the slope of the calibration line covering only the lower range, near the LOD (ICH, 2005).
387 It was 1.3 ng/g. The limit of quantification (LOQ) estimated as 3×LOD was 3.9 ng/g. The
388 R^2 value of the calibration line was 0.9913 and the residuals were lower than 20%.

389 *3.4. Influence of bioactive EVOH films on FB_2 production*

390 FB_2 levels in control and treated cultures at the end of the incubation period are
391 shown in Fig. 3, for EVOH-ORE and EVOH-CIN, and in Fig. 4 for the remaining
392 treatments. In control cultures of both isolates, FB_2 levels were significantly higher than
393 in treated cultures. Film type, dose, temperature, and a_w as well as all their interactions
394 has a very significant (p < 0.001) effect on FB_2 production. At 28 ºC the production of
395 FB_2 is greater than at 35 and 20 ºC for a given set of other factors. According to the
396 results of the effectiveness of the different films in controlling the growth of both isolates,
397 the films that produced the greatest reduction or total inhibition of FB_2 production was
398 EVOH-CINHO, followed by EVOH-IEG and EVOH-CIT. In EVOH-CINHO film treatments
399 incubated at 20 ºC, FB_2 was not detected, regardless of the dose and a_w. At 28 and 35
400 ºC and 0.99 or 0.97 a_w, FB_2 was detected only in the lowest dose treatments (250
401 µg/dish). Univariate analysis of variance of log transformed data [*log*(FB_2 conc.+1)]
402 indicated that isolate An2 produced significantly more FB_2 than isolate An14. Regarding

403 the main factors, the Tukey's test ($\alpha = 0.05$) found homogeneous groups for both isolates
404 (Table 5). For isolate An14, FB_2 levels increased in the treatments with the different
405 agents in the order CINHO < IEG < CIT < CAR < CIN < ORE < LIN, while for isolate An2
406 treatments the order was CINHO < IEG < CIT < ORE ≈ CIN, CIN ≈ CAR < LIN. Then
407 there was overlap with CIN, which was placed into two homogeneous groups. For both
408 isolates, the homogeneous groups designed for the factor dose were four, one for each
409 dose, and the most favorable temperature for FB_2 production was 28 ºC followed by 35
410 and 20 ºC. Regarding a_w, for isolate An14 there were three homogeneous groups and
411 the order from lower to higher FB_2 production was 0.95 < 0.99 < 0.97 a_w. For isolate An2,
412 there were two homogeneous groups and the order from lower to higher toxin production
413 was 0.95 < 0.99 ≈ 0.97 a_w.

414 *3.5. ML predictive models for GR and FB_2 production*

415 In the initial modeling approach, the variable "isolate" was excluded to assess the
416 differences in model performance with and without this input variable. In the subsequent
417 approach, "isolate" was included as a predictor. The output variables were the mean
418 values of GR, FB_2 concentration, and *log*(FB_2 concentration+1). The optimized
419 performance metrics (MSE and R^2) appear in Table 6.

420 XGBoost yielded the best performance for mean GR, exhibiting the lowest MSE
421 and highest R^2 for both isolated An2 and An14. The SVM model followed closely with
422 slightly reduced but comparable performance. Similarly, XGBoost provided the most
423 accurate models for both the mean *log*-transformed and mean raw FB_2 concentration,
424 offering a favorable balance between MSE and R^2. The second-best performances were
425 achieved by SVM or RF for the *log*-transformed output, and RF for the raw FB_2 data.
426 Both SVM and MLP were inadequate for predicting FB_2 concentration. XGBoost was the
427 most effective algorithm across all outputs. The regression lines of predicted *versus*
428 actual values for the best models using the test datasets are shown in Fig. 5.

When the “isolate” variable was included as an input, the SVM model demonstrated the highest accuracy for GR prediction (MSE = 0.0768, R^2 = 0.9511), with XGBoost showing comparable results. RF and MLP performed slightly worse, with R^2 values of 0.9063 and 0.9315, respectively (Table 6). Regression lines for the predicted versus actual values using the best-performing models are displayed in Fig. 5. For modeling mean FB_2 production, XGBoost again showed optimal performance using the *log*-transformed data (MSE = 0.1473, R^2 = 0.9044) (Table 6). Although this R^2 value is lower than that obtained for mean GR, it still indicates a strong predictive capacity. The RF model demonstrated reasonable predictive accuracy, aligning with the findings of XGBoost (Table 6). SVM exhibited a comparable performance profile, while MLP performed the worst. The use of FB_2 levels instead of the *log*-transformed as output was tested to evaluate model performance. In this case, only the model created using XGBoost showed an acceptable performance. RF accounted for the second place while SVM and MLP were unsuitable. Table 7 lists the hyperparameter values selected for the best ML models to predict as accurately as possible the three outputs.

4. Discussion

As shown in previous reports, the FB_2 production by *A. niger* isolates is high, although production levels are dependent on the specific isolate and the culture medium used. It was found that 39% of isolates from maize in Portugal produce FB_2 in the range of 1 to 5,382 ng/g on RC agar medium (Soares et al., 2013). In a study conducted in California, it was observed that 50% of isolates from vineyards produced FB_2 in the range of 1.2 to 27 µg/ml in CY20S medium (Palumbo et al., 2011). Seventy % of isolates from grapes cultivated in the Mediterranean region produce FB_2 at levels ranging from 0.5 to 3.3 µg/g in CY20S medium (Susca et al., 2014) and 77% of isolates from California, Argentina or Uganda raisins produce FB_2 at levels between 0.171 and 7.841 µg/g on grapes and raisins (Mogensen et al., 2010b). Logrieco et al. (2014) reported that 10 out of 17 samples of maize grains were contaminated by *Aspergillus* section *Nigri* with a

range from 6% to 68% of kernels. The ratio of FB_2/FB_1 contamination in the maize samples was evaluated and the highest values occurred in samples contaminated with *Aspergillus* section *Nigri*. All the *A. niger* isolates studied by Han et al. (2017) and used in the Chinese industry were found to be FB_2 producers on maize, rice and wheat bran at levels between 2 and 12,036 ng/g. *A. niger* has been widely used for the production of extracellular enzymes and organic acids for decades (Cairns et al., 2018, 2021). In our study on control cultures (not treated with bioactive films) of the two *A. niger* isolates from maize grains grown in Spain the mean levels of FB_2 produced in RC agar supplemented with different concentrations of NaCl ranged from 7 to 9,072 ng/g considering all the a_w and temperature conditions studied. These results are of great interest to the food industry, health, economics and biotechnology. FB_2 is a very common mycotoxin, especially in maize, and *A. niger* may be one of the major sources of the toxin in this cereal (Logrieco et al., 2014), and in other foods.

Despite the high percentage of *A. niger* isolates that are FB_2 producers, there are very few studies on the effect of external factors, such as antifungal agents or environmental conditions on the growth of FB_2-producing *A. niger* and FB_2 production. In only one report the effect of temperature and a_w on some strains of *A. niger* was investigated (Mogensen et al., 2009). These authors found that *A. niger* growth increased with higher temperature, with an optimum at 37 °C, followed by a slight decrease at 42 °C. The optimal a_w for growth was 0.99-0.98, and the growth was found to be partially inhibited below 0.98 a_w. These results are in agreement with those found in our study. The two tested *A. niger* isolates exhibited higher GR at 35 °C and 0.99 a_w. In contrast, the optimal temperature for the growth of ochratoxigenic strains of *A. niger* usually ranges between 24 and 37 ºC, with a_w levels ranging between 0.95 and 0.97 (Astoreca et al., 2007; Palacios-Cabrera et al., 2005; Passamani et al., 2014; Zhang et al., 2024). Therefore, the optimal temperature and a_w for *A. niger* growth are, in general, lower for ochratoxigenic isolates than for FB_2-producing isolates. This makes the latter strains

483 highly competitive in novel scenarios associated with climate change where elevated
484 temperatures persist.

485 The scarcity of prior research on the effect of EVOH films supplemented with EO/
486 EOC on *A. niger* growth and FB_2 production complicates the discussion our results.
487 Previous studies have demonstrated the efficacy of certain EO in controlling the growth
488 of this species. Nevertheless, there has been little research into their effect on mycotoxin
489 production or on the ED_{50}, ED_{90} and ED_{100}. *A. niger* growth can be completely inhibited
490 by the application of 200 ppm of thyme, 400 ppm of savory or 2400 ppm of sage EOs
491 (Jahani et al., 2020; Noshirvani and Fasihi, 2018) and cinnamon bark EO can produce a
492 zone of hyphal inhibition of 43 mm in a plate diffusion test (Pawar and Thaker, 2006). It
493 has been observed that carvacrol and thymol EOs encapsulated in MCM-41 (Mobil
494 Composition of Matter No. 41) maintain their antifungal activity and completely inhibit *A.*
495 *niger* growth (Bernardos et al., 2015). Furthermore, the encapsulation of cinnamon leaf
496 EO in nanoemulsions can significantly enhance the inhibitory effect against *A. niger*. As
497 demonstrated by Ribes et al. (2017), the radial mycelial growth is completely inhibited
498 by 0.25 μg/g of cinnamon leaf EO when nanoemulsions are utilized, whereas the same
499 concentration of free EO only reaches 75% inhibition (Ribes et al., 2017). Pineapple
500 nanocellulose and gellan gum films incorporated with *Apium graveolens* EO (2% and
501 4%) were evaluated as a means of bread packaging to inhibit *A. niger.* During three-
502 week storage period, no visible mycelial growth was detected (Sripahco et al., 2023).
503 The mechanism of the citral-eugenol combination against *A. niger* and its potential
504 application in extending bread shelf-life has been studied (Feng et al., 2025b; Ju et al.,
505 2020; Wang et al., 2024b). Eugenol was responsible for the permeability of damaged
506 cell membrane, whereas citral caused membrane lipid peroxidation. Their combination
507 revealed a synergistic inhibitory effect on *A. niger*. Carvacrol can induce apoptosis by
508 decreasing mitochondrial membrane potential in *A. flavus* (Duan et al., 2024). The star
509 anise EO inhibited *A. niger* growth by blocking the NAD synthetic pathway. Furthermore,
510 *A. niger* activated additional energy production pathways to compensate for the lack of
511 energy after the treatment (Zhao et al., 2022). CINHO could inhibit the ergosterol

synthesis of an *A. niger* strain isolated from spoiled paddy promoting malondialdehyde production and causing plasma membrane damage (Niu et al., 2022). CINHO can inhibit fungal growth by damaging cell ultrastructure and membrane integrity, by intracellular accumulation of ROS and induction of lipid oxidation and redox imbalance, although oxidative stress action could be the main mechanism by which CINHO exerts its antifungal effects against *A. niger* (Sun et al., 2020). In this framework, our results demonstrate that EVOH films supplemented with CINHO, IEG or CIT in the vapor phase can completely inhibit the growth of *A. niger* at doses in the ranges of 250-1500 µg/dish for CINHO, or 1000-4000 µg/dish, for IEG and CIT. Consequently, these films can serve as effective food packaging solutions for *A. niger* control in a wide range of temperatures (20-37 ºC) and a_w (0.96-0.99). The utilization of EVOH films containing CINHO, IEG, or CIT seems a highly recommended approach for the manufacture of multilayer coextruded films with LDPE, HDPE, PP or PET as packaging capable of preventing *A. niger* growth and FB_2 production in food products such as fresh cereal grains (maize, rice, wheat, etc.), fruits and vegetables (grapes, dates, tomatoes, etc.), or other foods, such as bread and cheese, which are often contaminated with *A. niger*.

The conditions for FB_2 production by *A. niger* have been little studied. In the study by Mogensen et al. (2009), the optimal temperature range was reported to be between 20 and 30 °C, with 25-30 °C being the most prevalent. The study also noted that the optimal a_w range was 0.985-0.97, depending on the strain. This finding is consistent with the results of our study, which show that the optimal FB_2 production by the two *A. niger* isolates occurred at 28 °C and 0.97 a_w. The optimal temperature for OTA production by *A. niger* is typically somewhat lower, ranging from 15 to 25 ºC (Passamani et al., 2014; Zhang et al., 2024). Consequently, the FB_2 risk in crops contaminated with *A. niger* appears to be elevated in warmer regions. It is important to highlight that the findings of this study show that FB_2 production did not correlate with fungal growth, as the maximum GR occurred at 0.99 a_w and 35 ºC, and the highest FB_2 levels occurred at 0.97 a_w and

539 28 ºC. Therefore, the factors a_w and temperature as well as their interactions, exert a
540 substantial influence on FB_2 production by *A. niger.*

541 In previous study on the efficacy of treatments with EVOH films supplemented
542 with different EOCs against *F. proliferatum*, the lowest EDs were recorded for EVOH-
543 CIT films at 28 ºC and 0.99 a_w, followed by EVOH-CINHO at 28 ºC and 0.96 a_w. The
544 factors film type and EOC dose significantly influenced FB_2 production, while
545 temperature and a_w showed no significant influence (Tarazona et al., 2021). In the
546 present study, CINHO, IEG, and CIT are also found to be highly effective in controlling
547 *A. niger* growth and FB_2 production, but the factors dosage, temperature and a_w exhibited
548 a significant effect on their efficacy. The findings of the present study demonstrate that,
549 at 20 °C and 35 °C, there was a decline in FB_2 production in comparison to 28 °C.
550 Similarly, FB_2 levels found at 0.95 and 0.99 a_w were significantly lower than those found
551 at 0.97 a_w in isolate An14 (Table 5).

552 Regarding the developed ML models, fungal GR prediction was achieved with
553 high accuracy using XGBoost and SVM, while RF also performed well. Both XGBoost
554 and SVM effectively model nonlinear relationships due to their ability to capture complex
555 variable dependencies. SVM is well-suited for small to medium-sized datasets and aims
556 to maximize the margin between predicted and actual values. XGBoost, based on
557 gradient boosting, iteratively combines weak learners to minimize prediction errors, while
558 incorporating regularization to reduce overfitting.

559 Although RF and MLP remain robust predictors, their relative lower performance
560 in this study may be attributed to specific limitations. RF may overfit in small or noisy
561 datasets due to lack of boosting mechanisms, while MLP requires extensive tuning and
562 is highly sensitive to architecture, especially when data is limited. This capacity is critical
563 in mycotoxin research where growth dynamics directly influence mycotoxin biosynthesis.
564 The strong performance of SVM and XGBoost highlights their suitability for modeling
565 fungal growth under varying environmental conditions. These predictive models can aid
566 in the design of strategies to mitigate fungal contamination, including optimizing

conditions in controlled environments. To date, no ML models have been developed for predicting *A. niger* growth in any medium. However, previous studies have demonstrated the effectiveness of XGBoost in modeling the growth of *Fusarium culmorum*, *F. graminearum* or *F. sporotrichioides* under bioactive films containing CINHO, CIT, IEG, and LIN (Mateo et al., 2021; Tarazona et al., 2021), which agrees with our results. Decision tree-based models, such as RF and XGB, have also shown strong predictive performance in estimating fungal productivity in forest ecosystems and have been recommended for future research in this domain (Morera et al., 2021). Additionally, various ML algorithms (ANN, XGBoost, SVM, and RF), have been successfully applied to predict the antifungal activity of gilaburu (*Viburnum opulus L.*) extract against eight *Fusarium* strains isolated from diseased potato tubers (Zangur et al., 2022). These findings confirm the reliability and cost-effectiveness of ML for antifungal modeling.

Concerning FB_2 production, XGBoost generated the best-performing models using both raw concentrations *and log*-transformed data, using the data sets for the two isolates together or separately. SVM and RF exhibited similar MSE and R^2 values with log-transformed data, with SVM performing slightly better for isolate An2. The relatively high MSE and low R^2 values of the models built with RF and, especially with SVM and MLP, for raw FB_2 levels compared to GR prediction are remarkable. As in the case of GR prediction, XGBoost again demonstrated superior performance. While RF and SVM performed well, they showed less accuracy than XGBoost. RF provides stability, but may not capture subtle data interactions. MLP's underperformance could be linked to its sensitivity to architecture, tuning, and overfitting when applied to high-dimensional data. Although ANNs can capture complex relationships, the dataset may not have been large or diverse enough for the MLP to generalize effectively without additional optimization. The main drawback of XGBoost is its computational intensity, as boosting is a sequential process requiring more resources than parallelizable methods such as RF (Inglis et al., 2024). SVM can be sensitive to outliers and kernel parameters selection. Applying a *log* transformation to FB_2 concentration improved model performance for by RF, SVM, and

595 MLP by reducing data variability, though XGBoost remained effective for both raw and
596 transformed outputs. Overall, XGBoost emerged as the most accurate and consistent
597 algorithm across all prediction tasks.

598 In a related study, XGBoost also outperformed decision tree, logistic regression,
599 SVM, in predicting the high-risk feed batches of agricultural commodities to be
600 considered for aflatoxin B_1 analysis (Wang et al., 2022), reinforcing its suitability for food
601 safety applications.

602 Accurately predicting mycotoxin production is crucial for assessing fungal
603 contamination risk in food and feed. The number of ML-based studies in this field is
604 increasing (Inglis et al., 2024) driven by the complexity of factors influencing toxin levels,
605 including fungal physiology and environmental variables. Reliable predictive models can
606 enhace early detection and mitigation strategies. The algorithms identified as most
607 effective in this study, particularly XGBoost and SVM, have strong potential for
608 integration into real-time monitoring systems, aiding in the prediction and prevention of
609 harmful contamination levels under diverse conditions.

610 **5. Conclusions**

611 To the best of our knowledge this study is the first to demonstrate the effects of
612 EVOH films incorporating selected EOs or their components (EOCs) on *A. niger* growth
613 and FB_2 production. The results underscore the significance of bioactive film design for
614 effective, natural antifungal strategies in food packaging. The efficacy of films with
615 CINHO was found to be the highest, followed by IEG, CIT, and CAR, while those with
616 CIN and LIN were found to be the least effective. Both GR and FB_2 levels decreased
617 with increasing EO/EOC doses. Fungal growth was favored at higher temperature and
618 a_w, whereas FB_2 production peaked at intermediates temperatures and high a_w. ED_{50} and
619 ED_{90} values generally increased with temperature and a_w. The interactions between the
620 variables considered (type of film, dose, temperature and a_w) imply that the reduction or
621 total inhibition of FB_2 production in the *A. niger* treatments is not always a direct
622 consequence of the reduction in fungal growth. Consequently, when formulating EVOH

films, it is imperative to take into account the impact of temperature and a_w. EVOH films with CINHO, IEG, or CIT are particularly promising for reducing *A. niger* GR and FB_2 production in susceptible foods including fresh cereals, fruits, bread and cheese. Among the four machine learning models tested, XGBoost provided the most accurate predictions of GR and FB_2 production. It was followed by SVM, which showed comparable or better performance in predicting GR under the evaluated conditions. Conversely, MLP proved to be the least effective.

Funding

The authors acknowledge financial support from the Ministry of Science, Innovation and Universities (Spanish Government) through Project PID2023-149211OB-C33.

Declaration of Competing Interest

The authors declare that they have no known competing financial interests or personal relationships that could have appeared to influence the present work.

References

Amézqueta, S., Schorr-Galindo, S., Murillo-Arbizu, M., González-Peñas, E., López de Cerain, A., Guiraud, J.P., 2012. OTA-producing fungi in foodstuffs: A review. Food Control 26, 259–268.

Andrade, P.A., 2023. Dietary risk assessment for fumonisins: challenges and prospects. Curr. Opin. Food Sci. 54, 101080.

Astoreca, A., Magnoli, C., Ramirez, M.L., Combina, M., Dalcero, A., 2007. Water activity and temperature effects on growth of *Aspergillus niger, A. awamori* and *A. carbonarius* isolated from different substrates in Argentina. Int. J. Food Microbiol. 119, 314-318.

Beccari, G., Stępień, Ł., Onofri, A., Lattanzio, V.M.T., Ciasca, B., Abd-El Fatah, S.I., Valente, F., Urbaniak, M., Covarelli, L., 2020**.** In vitro fumonisin biosynthesis and

genetic structure of *Fusarium verticillioides* strains from five Mediterranean countries. Microorganisms 8, 241.

Bernardos, A., Marina, T., Žáček, P., Pérez-Esteve, É., Martínez-Máñez, R., Lhotka, M., Kouřimská, L., Pulkrábek, J., Klouček P., 2015. Antifungal effect of essential oil components against *Aspergillus niger* when loaded into silica mesoporous supports. J. Sci. Food Agric. 95, 2824–2831.

Braun, M.S., Wink, M., 2018. Exposure, occurrence, and chemistry of fumonisins and their cryptic derivatives. Compr. Rev. Food Sci. Food. Saf. 17, 769–791.

Breiman, L., 2001. Random forests. Mach. Learn. 45, 5–32.

Bullerman, L.B., 1974. Screening medium and method to detect several mycotoxins in mold cultures. J. Milk Food Technol. 37, 1–3.

Cairns, T.C., Nai, C., Meyer, V., 2018. How a fungus shapes biotechnology: 100 years of *Aspergillus niger* research. Fungal Biol. Biotechnol. 5, 13.

Cairns, T.C., Barthel, L., Meyer, V., 2021. Something old, something new: challenges and developments in *Aspergillus niger* biotechnology. Essays Biochem. 65, 213–224.

Camardo Leggieri, M., Mazzoni, M., Battilani, P., 2021. Machine learning for predicting mycotoxin occurrence in maize. Front. Microbiol. 12, 661132.

Cerisuelo, J.P., Muriel-Galet, V., Bermúdez, J.M., Aucejo, S., Catalá, R., Gavara, R., Hernández-Muñoz, P., 2012. Mathematical model to describe the release of an antimicrobial agent from an active package constituted by carvacrol in a hydrophilic EVOH coating on a PP film. J. Food Eng. 110, 26–37.

Chen, T., Guestrin, C., 2016. XGBoost: a scalable tree boosting system. In: Proceedings of the 22nd ACM SIGKDD International Conference on Knowledge Discovery and Data Mining. San Francisco, CA, USA, pp. 785–794.

Chen, C., Riley, R.T., Wu, F., 2018. Dietary fumonisin and growth impairment in children and animals: a review. Compr. Rev. Food Sci. Food Saf. 17, 1448–1464.

Chiotta, M.L., Ponsone, M.L., Sosa, D.M., Combina, M., Chulze, S.N., 2013. Biodiversity of *Aspergillus* section *Nigri* populations in Argentinian vineyards and ochratoxin a contamination. Food Microbiol. 36, 182-190.

Commission Regulation (EU) 2023/915 of 25 April 2023 on maximum levels for certain contaminants in food and repealing Regulation (EC) No 1881/2006 (Text with EEA relevance) Official Journal of the European Union 5.5.2023. L 119, 103-157.

Copetti, M.V., Tamanaka, B.T., Pitt, J.I., Taniwaki M.H. 2014. Review. Fungi and mycotoxins in cocoa: From farm to chocolate. Int. J. Food Microbiol. 178, 13–20.

Cortes, C., Vapnik, V., 1995. Support-vector networks. Mach. Learn. 20, 273–297.

Desjardins, A.E., 2006. *Fusarium*, mycotoxins, chemistry. Genet. Biol. APS, St Paul, USA.

Duan, W., Zhu, X., Zhang, S., Lv, Y., Zhai, H., Wei, S., Ma, P., Hu, Y., 2024. Antifungal effects of carvacrol, the main volatile compound in *Origanum vulgare* L. essential oil, against *Aspergillus flavus* in postharvest wheat. Int. J. Food Microbiol. 410, 110514.

European Food Safety Authority (EFSA), 2007. Introduction of a qualified presumption of safety (QPS) approach for assessment of selected microorganisms referred to EFS (Question No EFSA-Q-2005-293). EFSA J. 2007, 587, 1-16.

European Food Safety Authority (EFSA), 2018. Appropriateness to set a group health-based guidance value for fumonisins and their modified forms. EFSA J. 16, 5172.

Farhadi, A., Fakhri, Y., Kachuei, R., Vasseghian, Y., Huseyn, E., Mousavi Khaneghah, A., 2021. Prevalence and concentration of fumonisins in cereal-based foods: a global systematic review and meta- analysis study. Environ. Sci. Pollut. Res. 28, 20998-21008.

Feng, Z., Shao, B., Yang, Q., Diao, Y., Ju, J. 2025a. The force of Zein self-assembled nanoparticles and the application of functional materials in food preservation. Food Chem. 463, 141197.

Feng, Z., Zhang, Q., Wang, Y., Yang, Q., Li, C., Zhao, F., Ju, J., 2025b. Anti-*Aspergillus niger* mechanism of small molecular combinations of essential oils and their application in extending the shelf-life of bread. Food Biosci. 64, 105979.

Ferranti, L.S., Fungaro, M.H.P., Massi, F.P., Silva, J.J.D., Penha, R.E.S., Frisvad, J.C., Taniwaki, M.H., Iamanaka, B.T., 2018. Diversity of *Aspergillus* section *Nigri* on the surface of *Vitis labrusca* and its hybrid grapes. Int. J. Food Microbiol. 268, 53–60.

Frisvad, J.C., Samson, R.A., 2004. Polyphasic taxonomy of *Penicillium* subgenus *Penicillium* - A guide to identification of food and airborne terverticillate Penicillia and their mycotoxins. Stud. Mycol. 49, 1-173.

Frisvad, J.C., Smedsgaard, J., Samson, R.A., Larsen, T.O., Thrane, U., 2007. Fumonisin B2 production by *Aspergillus niger.* J. Agric. Food Chem. 55*,* 9727–9732.

García-Cela, E., Crespo-Sempere, A., Gil-Serna, J., Porqueres, A., Marín, S., 2015. Fungal diversity, incidence and mycotoxin contamination in grapes from two agro-climatic Spanish regions with emphasis on *Aspergillus* species. J. Sci. Food Agric. 95, 1716-1729.

Gil-Serna, J., García-Díaz, M., Vázquez, C., González-Jaén, M.T., Patiño, B., 2019. Significance of *Aspergillus niger* aggregate species as contaminants of food products in Spain regarding their occurrence and their ability to produce mycotoxins. Food Microbiol. 82, 240-248.

Gil-Serna, J., Vázquez, C., González-Jaén, M.T., Patiño, B., 2018. Wine contamination with ochratoxins: a review. Beverages 4, 6.

Han, X., Jiang, H., Xu, J., Zhang, J., Li, F., 2017. Dynamic fumonisin B2 production by *Aspergillus niger* intended used in food industry in China. Toxins 9, 217.

ICH, International Committee on Harmonization, “Validation of Analytical Procedures: Text and Methodology”, Q2(R1). 2005.

Inglis, A., Parnell, A.C., Subramani, N., Doohan, F.M., 2024. Machine learning applied to the detection of mycotoxin in food: A systematic review. Toxins 16, 268.

727 Jahani, M., Pirab, M., Aminifard, M.H., 2020. Antifungal effects of essential oils against
728 *Aspergillus niger* in vitro and in vivo on pomegranate (*Punica granatum*) fruits. Sci.
729 Hortic. 264, 109188.
730 Ju, J., Xie, Y., Yu, H., Guo, Y., Cheng, Y., Zhang, R., Yao, W., 2020. Synergistic inhibition
731 effect of citral and eugenol against *Aspergillus niger* and their application in bread
732 preservation. Food Chem., 310, 125974.
733 Junior, O.F.R., Dalcin, M.S., Nascimento, V.L., Haesbaert, F.M., Ferreira, T.P.d.S.,
734 Fidelis, R.R., Sarmento, R.d.A., Aguiar, R.W.d.S., Oliveira, E.E.d., Santos, G.R.d.,
735 2019. Fumonisin production by *Fusarium verticillioides* in maize genotypes cultivated
736 in different environments. Toxins 11, 215.
737 Kigen, G., Busakhala, N., Kamuren, Z., Rono, H., Kimalat, W., Njiru, E., 2017. Factors
738 associated with the high prevalence of oesophageal cancer in Western Kenya: a
739 review. Infect. Agent. Cancer 12, 59.
740 Knudsen, P.B., Mogensen, J.M., Larsen, T.O., Nielsen, K.F., 2010. Occurrence of
741 fumonisins B2 and B4 in retail raisins. J. Agric. Food Chem. 59, 772-776.
742 Lee, H.J., Ryu, D., 2017. Worldwide occurrence of mycotoxins in cereals and cereal-
743 derived food products: public health perspectives of their co-occurrence. J. Agric.
744 Food Chem. 65, 7034–7051.
745 Liaw A., Wiener, M.C., 2002. Classification and regression by randomForest. R News 2,
746 18–22.
747 Logrieco, A., Ferracane, R., Haidukowsky, M., Cozzi, G., Visconti, A., Ritieni, A., 2009.
748 Fumonisin B_2 production by *Aspergillus niger* from grapes and natural occurrence in
749 must. Food Addit. Contam. Part A. 26, 1495–1500.
750 Logrieco, A., Ferracane, R., Visconti, A., Ritieni, A., 2010. Natural occurrence of
751 fumonisin B_2 in red wine from Italy. Food Addit. Contam. Part A. 27, 1136–1141.
752 Logrieco, A.F., Haidukowski, M., Susca, A., Mulè, G., Munkvold, G.P., Moretti, A., 2014.
753 *Aspergillus* section *Nigri* as contributor of fumonisin B2 contamination in maize. Food
754 Addit. Contam. Part A. 31, 149–155.

Luzi, F., Torre, L., Puglia, D., 2020. Antioxidant packaging films based on ethylene vinyl alcohol copolymer (EVOH) and caffeic acid. Molecules 25*, 3953.*

Mansson, M., Klejnstrup, M.L., Phipps, R.K., Nielsen, K.F., Frisvad, J.C., Gotfredsen, C.H., Larsen, T.O., 2009. Isolation and NMR characterization of fumonisin B2 and a new fumonisin B6 from *Aspergillus niger*. J. Agric. Food Chem. 58, 949–953.

Marasas, W.F.O., Jaskiewicz, K., Venter, F.S., van Schalkwyk, D.J., 1988. *Fusarium moniliforme* contamination of maize in esophageal cancer areas in Transkei. South Afr. Med. J. 74, 110–114.

Mateo, R., Medina, A., Mateo, E.M., Mateo, F., Jiménez, M., 2007. An overview of ochratoxin A in beer and wine. Int. J. Food Microbiol. 119, 79–83.

Mateo, E.M., Gómez J.V., Domínguez, I., Gimeno-Adelantado, J.V., Mateo-Castro, R., Gavara, R., Jiménez, M., 2017. Impact of bioactive packaging systems based on EVOH films and essential oils in the control of aflatoxigenic fungi and aflatoxin production in maize. Int. J. Food Microbiol. 254, 36–46.

Mateo, E.M., Gómez, J.V., Tarazona, A., García-Esparza, M.Á., Mateo, F., 2021. Comparative analysis of machine learning methods to predict growth of *F. sporotrichioide*s and production of T-2 and HT-2 toxins in treatments with ethylene-vinyl alcohol films containing pure components of essential oils. Toxins 13, 545.

Mogensen, J.M., Nielsen, N.K., Samson, R.A., Frisvad, J.C., Thrane, U., 2009. Effect of temperature and water activity on the production of fumonisins by *Aspergillus niger* and different *Fusarium* species. BMC Microbiol. 9, 281.

Mogensen, J.M., Frisvad, J.C., Thrane, U., Nielsen, K.F., 2010a. Production of fumonisin B2 and B4 by *Aspergillus niger* on grapes and raisins. J. Agric. Food Chem. 2010a, 58, 954–958.

Mogensen, J.M., Larsen, T.O., Nielsen, K.F. 2010b. Widespread occurrence of the mycotoxin fumonisin B_2 in wine. J. Agric. Food Chem. 58, 4853–4857.

Morera, A., Martínez de Aragón, J., Bonet, J.A., Liang, J., de-Miguel S., 2021. Performance of statistical and machine learning-based methods for predicting

biogeographical patterns of fungal productivity in forest ecosystems. For. Ecosyst. 8, 21.

Muriel-Galet, V., López-Carballo, G., Hernández-Muñoz, P., Gavara, R., 2014. Characterization of ethylene-vinyl alcohol copolymer containing lauril arginate (LAE) as material for active antimicrobial food packaging. Food Pack. Shelf Life 1, 10-18.

Muriel-Galet, V., Cran, M.J., Bigger, S.W., Hernández-Muñoz, P., Gavara, R., 2015. Antioxidant and antimicrobial properties of ethylene vinyl alcohol copolymer films based on the release of oregano essential oil and green tea extract components. J. Food Eng. 149, 9–16.

Nelson, P.E., Plattner, R.D., Shackelford, D.D., Desjardins, A.E., 1992. Fumonisin B_1 production by *Fusarium* species other than *F. moniliforme* in Section Liseola and by some related species. Appl. Environ. Microbiol. 58, 984–989.

Niu, A., Wu, H., Ma, F., Tan, S., Wang, G., Qiu, W., 2022. The antifungal activity of cinnamaldehyde in vapor phase against *Aspergillus niger* isolated from spoiled paddy. LWT, 159, 113181.

Noonim, P., Mahakarnchanakul, W., Nielsen, K.F., Frisvad, J.C., Samson, R.A., 2009. Fumonisin B2 production by *Aspergillus niger* in Thai coffee beans. Food Addit. Contam. 26, 94–100.

Noshirvani, N., Fasihi, H., 2018. Control of *Aspergillus niger* in vitro and in vivo by three Iranian essential oils. Int. Food Res. J. 25, 1745–1752.

Palacios-Cabrera, H., Taniwaki, M.H., Hashimoto, J.M., de Menezes. H.C., 2005. Growth of *Aspergillus ochraceus, A. carbonarius* and *A. niger* on culture media at different water activities and temperatures. Braz. J. Microbiol. 36, 24-28.

Palumbo, J.D., O'keeffe, T.L., Ho, I.S., Fidelibus, M.W., 2016. Population dynamics of *Aspergillus* section *Nigri* species on vineyard samples of grapes and raisins. J. Food Prot. 79, 448–453.

809 Palumbo, J.D., O'keeffe, T.L., Mcgarvey, J.A., 2011. Incidence of fumonisin B2
810 production within Aspergillus section *Nigri* populations isolated from California raisins.
811 J. Food Prot. 74, 672–675.
812 Pantelides, I.S., Aristeidou, E., Lazari, M., Tsolakidou, M.D., Tsaltas, D., Christofidou,
813 M., Kafouris, D., Christou. E., Ioannou, N., 2017. Biodiversity and ochratoxin A profile
814 of *Aspergillus* section *Nigri* populations isolated from wine grapes in Cyprus
815 vineyards. Food Microbiol. 67, 106–115.
816 Passamani, F.R., Hernandes, T., Lopes, N.A., Bastos, S.C., Santiago, W.D., Cardoso,
817 Md., Batista, L.R., 2014. Effect of temperature, water activity, and pH on growth and
818 production of ochratoxin A by *Aspergillus niger* and *Aspergillus carbonarius* from
819 Brazilian grapes. J. Food Prot. 77, 1947–52.
820 Pawar, V.C., Thaker, V.S., 2006. In vitro efficacy of 75 essential oils against *Aspergillus*
821 *niger.* Mycoses 49, 316–323.
822 Pedregosa, F., Varoquaux, G., Gramfort, A., Michel, V., Thirion, B., Grisel, O., et al. 2011.
823 Scikit-learn: Machine learning in Python. J. Mach. Learn. Res. 12, 2825–2830.
824 Periasamy, V.S., Athinarayanan, J., Alshatwi, A.A., 2016. Anticancer activity of an
825 ultrasonic nanoemulsion formulation of *Nigella sativa* L. essential oil on human breast
826 cancer cells. Ultrason. Sonochem. 31, 449–455.
827 Perrone, G., De Girolamo, A., Sarigiannis, Y., Haidukowski, M.E., Visconti, A., 2013.
828 Occurrence of ochratoxin *A*, fumonisin B2 and black aspergilli in raisins from western
829 Greece regions in relation to environmental and geographical factors. Food Addit.
830 Contam. Part. A. 30, 1339–1347.
831 Qi, T.F., Renaud, J.B., McDowell, T., Seifert, K.A., Yeung, K.K.C., Sumarah, M.W., 2016.
832 Diversity of mycotoxin-producing black aspergilli in Canadian vineyards. J. Agric.
833 Food Chem. 64, 1583–1589.
834 Qu, K., Guo, F., Liu, X., Lin, Y., Zou, Q., 2019. Application of machine learning in
835 Microbiology. Front. Microbiol. 10, 827.

836 Qu, L., Wang, L., Ji, H., Fang, Y., Lei, P., Zhang, X., Jin, L., Sun, D., Dong, H., 2022.
837 Toxic mechanism and biological detoxification of fumonisins. Toxins 14, 182.
838 Rheeder, J.P., Marasas, W.F., Vismer, H.F., 2002. Production of fumonisin analogs by
839 *Fusarium* species. Appl. Environ. Microbiol. 68, 2101–2105.
840 Ribes, S., Fuentes, A., Talens, P., Barat, J.M., Ferrari, G., Donsì, F., 2017. Influence of
841 emulsifier type on the antifungal activity of cinnamon leaf, lemon and bergamot oil
842 nanoemulsions against *Aspergillus niger*. Food Control 73, 784–795.
843 Rumelhart, D.E., Hinton, G.E., Williams, R.J., 1986. Learning representations by back-
844 propagating errors. Nature 323(6088), 533–536.
845 Samson, R.A., Hoekstra, E.S., Frisvad, J.C., 2004. Introduction to food and airborne
846 fungi. 7th edition. Utrecht, the Netherlands: Centralbureau voor Schimmel cultures.
847 Samson, R.A., Noonim, P., Meijer, M., Houbraken, J., Frisvad, J.C., Varga, J., 2007.
848 Diagnostic tools to identify black aspergilli. Stud. Mycol. 59, 129-145.
849 Shelke, Y.P., Badge, A.K., Bankar, N.J., 2023. Applications of artificial intelligence in
850 microbial diagnosis. Cureus 15, 49366.
851 Smith, K.P., Wang, H., Durant, T.J., Mathison, B.A., Sharp, S.E., Kirby, J.E., Long, S.W.,
852 Rhoads, D.D., 2020. Applications of artificial intelligence in clinical microbiology
853 diagnostic testing. Clin. Microbiol. Newsl. 42, 61–70.
854 Soares, C., Calado, T., Venâncio, A., 2013. Mycotoxin production by *Aspergillus niger*
855 aggregate strains isolated from harvested maize in three Portuguese regions. Rev.
856 Iberoam. Micol. 30, 9–13.
857 Sripahco, T., Khruengsai, S., Pripdeevech, P., 2023. Biodegradable antifungal films from
858 nanocellulose-gellan gum incorporated with *Anethum graveolens* essential oil for
859 bread packaging. Int. J. Biol. Macromol. 243,125244.
860 Stępień, L., Koczyk, G., Waśkiewicz, A., 2011. Genetic and phenotypic variation of
861 *Fusarium proliferatum* isolates from different host species. J. Appl. Genet. 52, 487–
862 496.

Sun, Q., Li, J., Sun, Y., Chen, Q., Zhang, L., Le, T., 2020. The antifungal effects of cinnamaldehyde against *Aspergillus niger* and its application in bread preservation, Food Chem. 317, 126405.

Susca, A., Proctor, R.H., Butchko, R.A.E., Haidukowski, M., Stea, G., Logrieco, A., Moretti, A., 2014. Variation in the fumonisin biosynthetic gene cluster in fumonisin-producing and nonproducing black aspergilli. Fungal Genet. Biol. 73, 39–52.

Tarazona, A., Gómez, J.V., Gavara, R., Mateo-Castro, R., Gimeno-Adelantado, J.V., Jiménez, M., Mateo. E.M., 2018. Risk management of ochratoxigenic fungi and ochratoxin A in maize grains by bioactive EVOH films containing individual components of some essential oils. Int. J. Food Microbiol. 269, 107-119,

Tarazona, A., Gómez, J.V., Mateo, F., Jiménez, M., Romera, D., Mateo, E.M., 2020. Study on mycotoxin contamination of maize kernels in Spain. Food Control 118, 107370.

Tarazona, A., Mateo, E.M., Gómez, J.V., Gavara, R., Jiménez, M., Mateo, F., 2021. Machine learning approach for predicting *Fusarium culmorum* and *F. proliferatum* growth and mycotoxin production in treatments with ethylene-vinyl alcohol copolymer films containing pure components of essential oils. Int. J. Food Microbiol. 338, 109012.

Varga, J., Kocsubé, S., Suri, K., Szigeti, G., Szekeres, A., Varga, M., Tóth, B., Bartók, T., 2010. Fumonisin contamination and fumonisin producing black Aspergilli in dried vine fruits of different origin. Int. J. Food Microbiol. 143, 143–149.

Wang, X., Bouzembrak, Y., Oude Lansink, A.G.J.M., van der Fels-Klerx, H.J., 2022. Designing a monitoring program for aflatoxin B1 in feed products using machine learning. npj Sci. Food 6, 40.

Wang, J., Gao, Q., Zhao, F., Ju, J., 2024a. Repair mechanism and application of self-healing materials for food preservation. Crit. Rev. Food Sci. Nutr. 64, 11113–11123.

Wang, J., Yang, Q., Zhao, F., Li, M., Ju, J., 2024b. Synergistic antifungal mechanism of eugenol and citral against *Aspergillus niger*: Molecular Level. Ind. Crop Prod. 213, 118435.

Yang, D., Ye, Y., Sun, J., Wang, J.S., Huang, C., Sun, X., 2022. Occurrence, transformation and toxicity of fumonisins and their covert products during food processing. Crit. Rev. Food Sci. Nutr. 14, 1–14.

Yen, H.F., Hsieh, C.T., Hsieh, T.J., Chang, F.R., Wang, C.K., 2015. In vitro antidiabetic effect and chemical component analysis of 29 essential oils products. J. Food Drug Anal. 23, 124–129.

Zhang, Y., Zhang, Z., Xu, Q., Lv, Y., Zhang, S., Zhai, H., Hu, Y., Wei, S., 2024. Effects of temperature on the production of ochratoxin A by *Aspergillus niger*. LWT Food Sci. Technol. 191, 115684.

Zhao, F., Huang, J., Qi, J., Li, Q., Wu, H., Ju, J., 2022. Proteomic analysis of antifungal mechanism of star anise essential oil against *Aspergillus niger* and its application potential in prolonging bread shelf life. LWT Food Sci. Technol. 169, 114023.

Zongur, A., Kavuncuoglu, H., Kavuncuoglu, E., Dursun Capar, T., Yalcin, H., Akif Buzpinar, M., 2022. Machine learning approach for predicting the antifungal effect of gilaburu (*Viburnum opulus*) fruit extracts on *Fusarium* spp. isolated from diseased potato tubers. J. Microbiol. Meth. 192, 106379.

908 **Figure captions**

909 Fig. 1. Mean GR of *A. niger* isolates An2 and An14 cultured on RC agar with EVOH-ORE
910 and EVOH-CIN films at four doses (250, 1000, 1500 and 4000 µg/dish) under nine
911 different combinations temperature/a_w. GR observed in culture controls are also
912 shown. Error bars are omitted for clarity (0 to 0.3 mm/day).

913 Fig. 2. Mean GR of *A. niger* isolates An2 and An14 cultured on RC agar with EVOH-
914 CAR, EVOH-CINHO, EVOH-CIT, EVOH-IEG and EVOH-LIN films at four doses (250,
915 1000, 1500 and 4000 µg/dish) under nine different combinations temperature/a_w. GR
916 observed in control cultures are also shown. Error bars are omitted for clarity.

917 Fig. 3. Mean FB_2 concentrations in RC agar cultures of *A. niger* isolates An2 and An14
918 under treatments with EVOH-ORE and EVOH-CIN at four doses (250, 1000, 1500
919 and 4000 µg/dish) and nine different combinations temperature/aw. FB_2 levels in
920 control cultures are also shown. Error bars mean standard errors.

921 Fig. 4. Mean FB_2 concentrations in RC agar cultures of *A. niger* isolates An2 and An14
922 under treatments with EVOH-CAR, EVOH-CINHO, EVOH-CIT, EVOH-IEG and
923 EVOH-LIN at four doses (250, 1000, 1500 and 4000 µg/dish) and nine different
924 combinations temperature/aw. FB_2 levels in control cultures are also shown. Error
925 bars mean standard errors.

926 Fig. 5. Linear regression plots of predicted *versus* actual mean values for GR, FB_2
927 concentration, *log*(FB_2 concentration+1) of the two *A. niger* isolates (An2 and An14)
928 and both together (An2 + An14) generated by the most accurate predictive ML models
929 for the test sets. The best algorithm appears on the top of each plot.

Table 1. Algorithms, hyperparmeters and their tested values for the design of machine learning (ML) models for prediction of *Aspergillus niger* growth rate and FB_2 production.

Algorithm [a]	Hyperparameter	Values
XGBoost	n_estimators	100, 200, 300, 500
	learning_rate	0.01, 0.05, 0.1, 0.2
	max_depth	3, 5, 7, 10
	subsample	0.8, 1.0
	colsample_bytree	0.8, 1.0
RF	n_estimators	100, 200, 300, 500
	max_depth	None, 10, 20, 30
	min_samples_split	2, 5, 10
	min_samples_leaf	1, 2, 5
	max_features	sqrt, log2
SVM	C	0.1, 1, 10, 100
	epsilon	0.01, 0.1, 1
	kernel	linear, rbf
	gamma	scale, auto, 0.01, 0.1, 1
MLP	hidden_layer_sizes	(50), (50, 50), (100), (100, 50)
	activation	relu, tanh, logistic
	alpha	0.0001, 0.001, 0.01, 0.1
	max_iter	500

[a] XGBoost: extreme gradient boosting tree; RF; random foresst; SVM: support vector machine; MLP: multilayer perceptor neural network

Table 2. Classification in homogeneous groups of bioactive EVOH film types, doses, temperatures and water activities concerningg their effects on the growth rate of two *A. niger* isolates by Tukey's HSD test.

		Isolate of *A. niger*			
		An2		An14	
		Growth rate		Growth rate	
Factor	Level	Low	High	Low	High
Bioactive EVOH film type	CINHO	•		•	
	IEG	•		•	
	CIT	•		•	
	CAR		•		•
	ORE		•		•
	CIN		•		•
	LIN		•		•
Dose (µg EO/Petri dish)	4000	•		•	
	1500	•		•	
	1000		•		•
	250		•		•
Temperature (º C)	20	•		•	
	28	•		•	
	35		•		•
Water activity	0.95	•		•	
	0.97	•		•	
	0.99		•		•

Within each column, levels containing a black circle form a group of means within which Tukey's HSD test finds no statistically significant differences (α = 0.05).

Table 3. Mean effective doses (ED_{50}, ED_{90} and ED_{100}) (µg/Petri dish) of oregano (ORE) and cinnamon bark (CIN) essential oils in EVOH films to control the growth of two *Aspergillus niger* isolates on RC agar under different conditions of temperature and a_w.

Antifungal agent	Temp. (ºC)	a_w	**Isolate An2**			**Isolate An14**		
			ED_{50}	ED_{90}	ED_{100}	ED_{50}	ED_{90}	ED_{100}
EVOH-ORE	20	0.99	740	>4000	>4000	750	>4000	>4000
		0.97	542	>4000	>4000	641	3990	>4000
		0.95	248	1245	1500	244	1099	1500
	28	0.99	1330	>4000	>4000	875	3810	>4000
		0.97	1133	>4000	>4000	670	3705	>4000
		0.95	620	>4000	>4000	245	3030	4000
	35	0.99	1438	>4000	>4000	1451	>4000	>4000
		0.97	1336	>4000	>4000	820	>4000	>4000
		0.95	905	>4000	>4000	535	>4000	>4000
EVOH-CIN	20	0.99	1503	>4000	>4000	1100	>4000	>4000
		0.97	1410	>4000	>4000	810	3950	>4000
		0.95	243	1250	1500	170	1040	1500
	28	0.99	2365	>4000	>4000	1130	>4000	>4000
		0.97	1137	>4000	>4000	880	>4000	>4000
		0.95	1000	>4000	>4000	755	>4000	>4000
	35	0.99	2680	>4000	>4000	2310	>4000	>4000
		0.97	1315	3370	4000	891	>4000	>4000
		0.95	880	1390	1500	760	3110	>4000

Table 4. Mean effective doses (ED_{50}, ED_{90} and ED_{100}) (µg/Petri dish) of pure components of essential oils (carvacrol, cinnamaldehyde, citral, isoeugenol and linalool) in EVOH films to control the growth of two *Aspergillus niger* isolates on RC agar under different conditions of temperature and a_w.

Antifungal agent	Temp. (ºC)	a_w	Isolate An2			Isolate An14		
			ED_{50}	ED_{90}	ED_{100}	ED_{50}	ED_{90}	ED_{100}
EVOH-CAR	20	0.99	240	1500	3960	250	2800	4000
		0.97	230	1245	1500	225	1390	1500
		0.95	180	750	1000	140	290	1000
	28	0.99	1275	>4000	>4000	950	>4000	>4000
		0.97	950	>4000	>4000	463	3990	>4000
		0.95	540	>4000	>4000	250	1105	1500
	35	0.99	2750	>4000	>4000	1090	>4000	>4000
		0.97	1460	>4000	>4000	750	>4000	>4000
		0.95	850	>4000	>4000	440	>4000	>4000
EVOH-CINHO	20	0.99	145	240	1000	140	234	1000
		0.97	125	225	250	120	215	250
		0.95	120	215	250	124	220	250
	28	0.99	200	1210	1500	170	715	1000
		0.97	180	1020	1500	165	700	1000
		0.95	120	225	250	119	220	250
	35	0.99	220	1230	1500	175	995	1500
		0.97	175	1070	1500	170	705	1000
		0.95	125	220	250	125	225	250
EVOH-CIT	20	0.99	430	3000	4000	500	2100	4000
		0.97	350	1310	1500	350	1250	1500
		0.95	175	740	1000	140	300	1000
	28	0.99	745	3305	4000	875	2750	4000
		0.97	540	2910	4000	530	2610	4000
		0.95	250	1450	4000	178	750	1000
	35	0.99	1310	3350	4000	1275	3300	4000
		0.97	925	3185	4000	805	2958	4000
		0.95	540	1430	4000	390	1310	1500
EVOH-IEG	20	0.99	717	1500	4000	675	1325	1500
		0.97	440	1250	1500	635	1315	1500
		0.95	210	808	1000	165	660	1000
	28	0.99	880	2250	4000	760	1750	4000
		0.97	525	1440	4000	610	1500	4000
		0.95	400	1400	4000	365	1352	4000
	35	0.99	750	2380	4000	840	2190	4000
		0.97	620	2140	4000	675	1710	4000
		0.95	520	2005	4000	520	1660	4000
EVOH-LIN	20	0.99	1500	>4000	>4000	1500	>4000	>4000
		0.97	905	>4000	>4000	1180	>4000	>4000
		0.95	525	910	1000	500	890	1000
	28	0.99	2200	>4000	>4000	1600	>4000	>4000
		0.97	1150	>4000	>4000	1250	>4000	>4000
		0.95	875	>4000	>4000	740	>4000	>4000
	35	0.99	2380	>4000	>4000	1460	>4000	>4000
		0.97	1417	>4000	>4000	1340	>4000	>4000
		0.95	1115	>4000	>4000	1050	>4000	>4000

Table 5. Classification in homogeneous groups of bioactive EVOH film types, doses, temperatures and water activities concerning their effects on FB_2 production of two *A. niger* isolates by Tukey's HSD test.

		Fungal isolate of *A. niger*			
		An2		An14	
		Log(conc. FB_2+1) [a]		*Log*(conc. FB_2+1) [a]	
Factor	Level	Low	High	Low	High
Bioactive EVOH film	CINHO	•		•	
	IEG	•		•	
	CIT	•		•	
	CAR		•		•
	CIN	•	•		•
	ORE	•			•
	LIN		•		•
Dose (µg EO/EOC per Petri dish)	4000	•		•	
	1500	•		•	
	1000	•		•	
	250		•		•
Temperature (º C)	20	•		•	
	28		•		•
	35	•		•	
Water activity	0.95	•		•	
	0.97	•		•	
	0.99	•			•

[a] The decimal logarithm of the FB_2 concentration plus 1 was used.
Within each column, levels containing a black circle form a group of means within which Tukey's HSD test finds no statistically significant differences (α = 0.05). Black circles in the same row mean overlap.

Table 6. Performance of the best machine learning (ML) models generated by four algorithms for predicting the growth rate (GR), of the *A. niger* isolates, FB_2 concentration and *log*(FB_2 concentration + 1) on the test set.

		Output variable					
		Mean GR		Mean FB_2 level		Mean *log*(FB_2+1) [a]	
Dataset	Algorithm	MSE [b]	R^2	MSE	R^2	MSE	R^2
An2	XGBoost [c]	0.12823	0.95073	5230	0.97748	0.14109	0.92593
	RF [d]	0.32672	0.87446	353075	0.84797	0.23654	0.87582
	SVM [e]	0.12895	0.95045	2034272	0.12411	0.16067	0.91565
	MLP [f]	0.42042	0.83846	1748013	0.24736	0.45971	0.75865
An14	XGBoost	0.09778	0.94034	4821	0.99068	0.11159	0.92389
	RF	0.22963	0.85989	109094	0.78921	0.18035	0.87699
	SVM	0.11638	0.92898	418738	0.19092	0.18823	0.87162
	MLP	0.44162	0.73055	396900	0.23312	0.71754	0.51062
An2+ An14	XGBoost	0.08355	0.94685	41179	0.96485	0.14733	0.90437
	RF	0.14731	0.9062	160722	0.86282	0.18989	0.87675
	SVM	0.07684	0.95112	913336	0.22048	0.18213	0.88179
	MLP	0.10776	0.93146	916013	0.21819	0.24830	0.83884

[a] Mean decimal *log* of FB_2 concentration plus 1; [b] MSE: Mean square error; [c] Extreme gradient boosted tree; [d] Random forest; [e] Support vector machine; [f] Multiple layer perceptron neural network.

Table 7. Hyperparameter values of the best ML models for predicting growth rate (GR) of *Aspergillus niger isolates* and FB_2 production.

	Isolates								
	An2			An14			An2+An14		
	Output			Output			Output		
	GR	FB_2 [a]	*Log*(FB_2+1) [b]	GR	FB_2	*Log*(FB_2+1)	GR	FB_2	*Log*(FB_2+1)
Best algorithm	XGBoost	XGBoost	XGBoost	XGBoost	XGBoost	XGBoost	SVM	XGBoost	XGBoost
Hyperparameter [c]									
– colsample_bytree	1.0	1.0	1.0	0.8	1.0	1.0		0.8	1.0
– learning_rate	0.05	0.05	0.1	0.1	0.05	0.05		0.2	0.05
– max_depth	3	7	10	3	10	10		5	10
– n_estimators	500	200	100	300	200	200		100	200
– subsample	0.8	0.8	0.8	0.8	1.0	0.8		1.0	0.8
– C							10		
– epsilon							0.1		
– gamma							0.1		
– kernel							rbf		

[a] Mean FB_2 concentration; [b] mean decimal logarithm of FB_2 concentration plus 1; [c] See Table 1

Figure 1

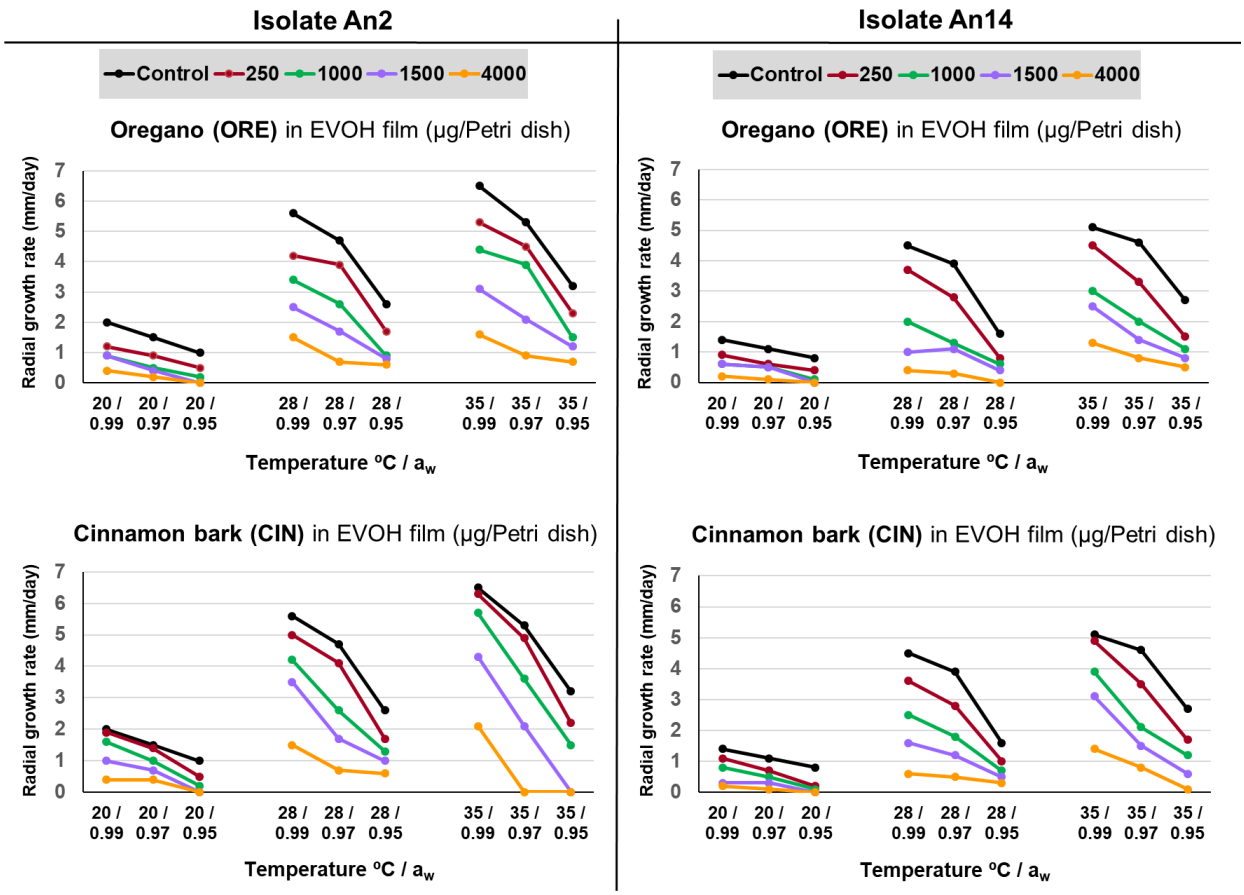

Figure 2

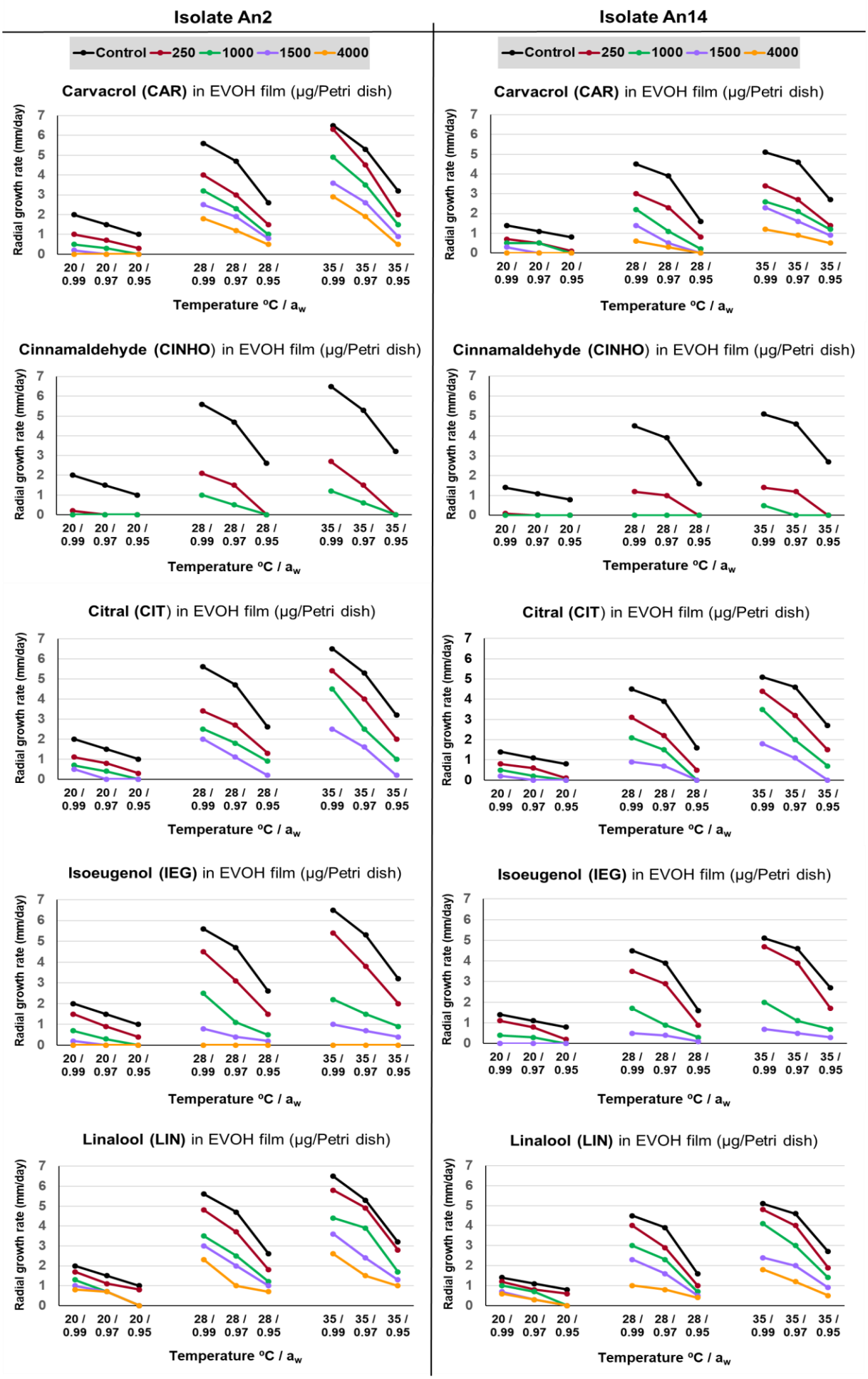

Figure 3

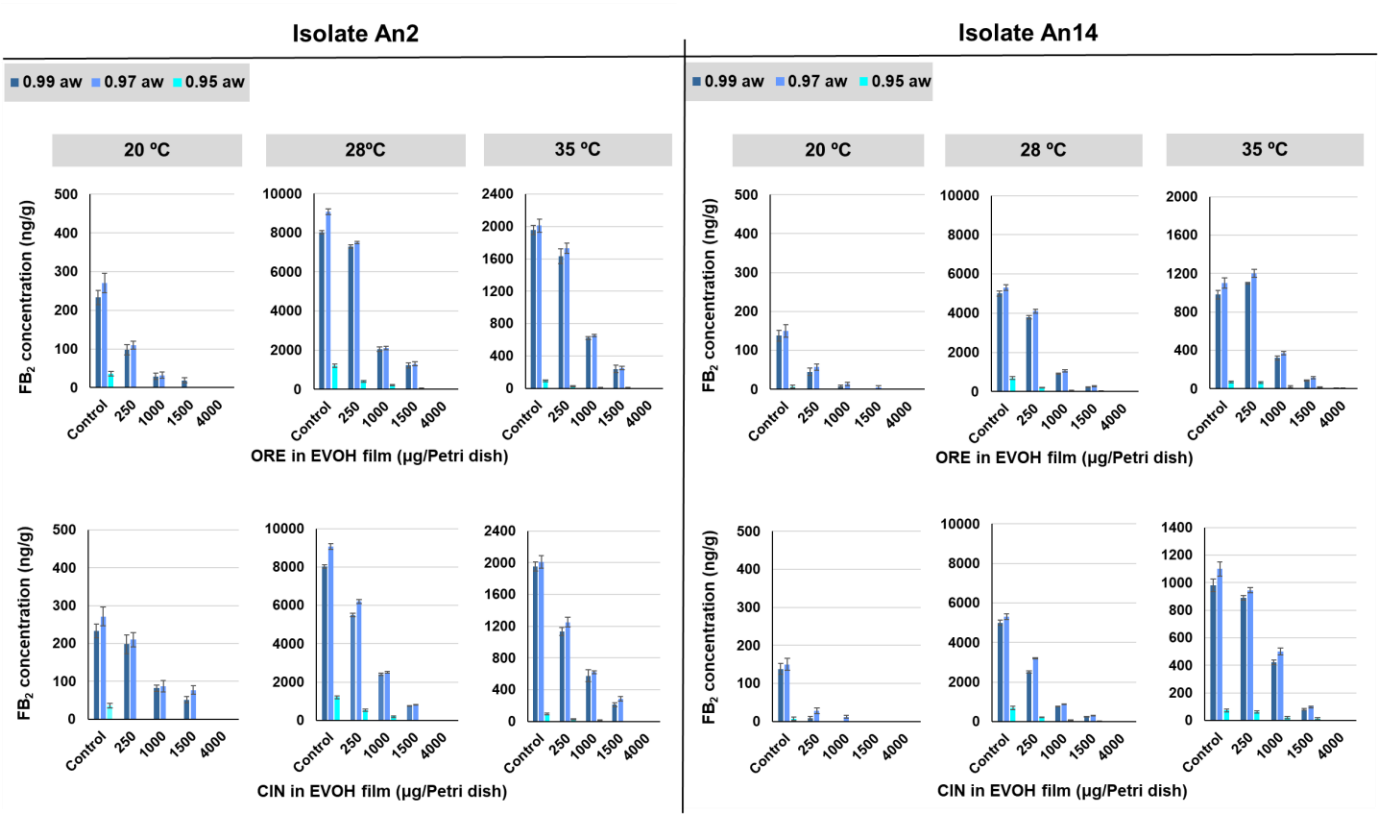

Figure 4

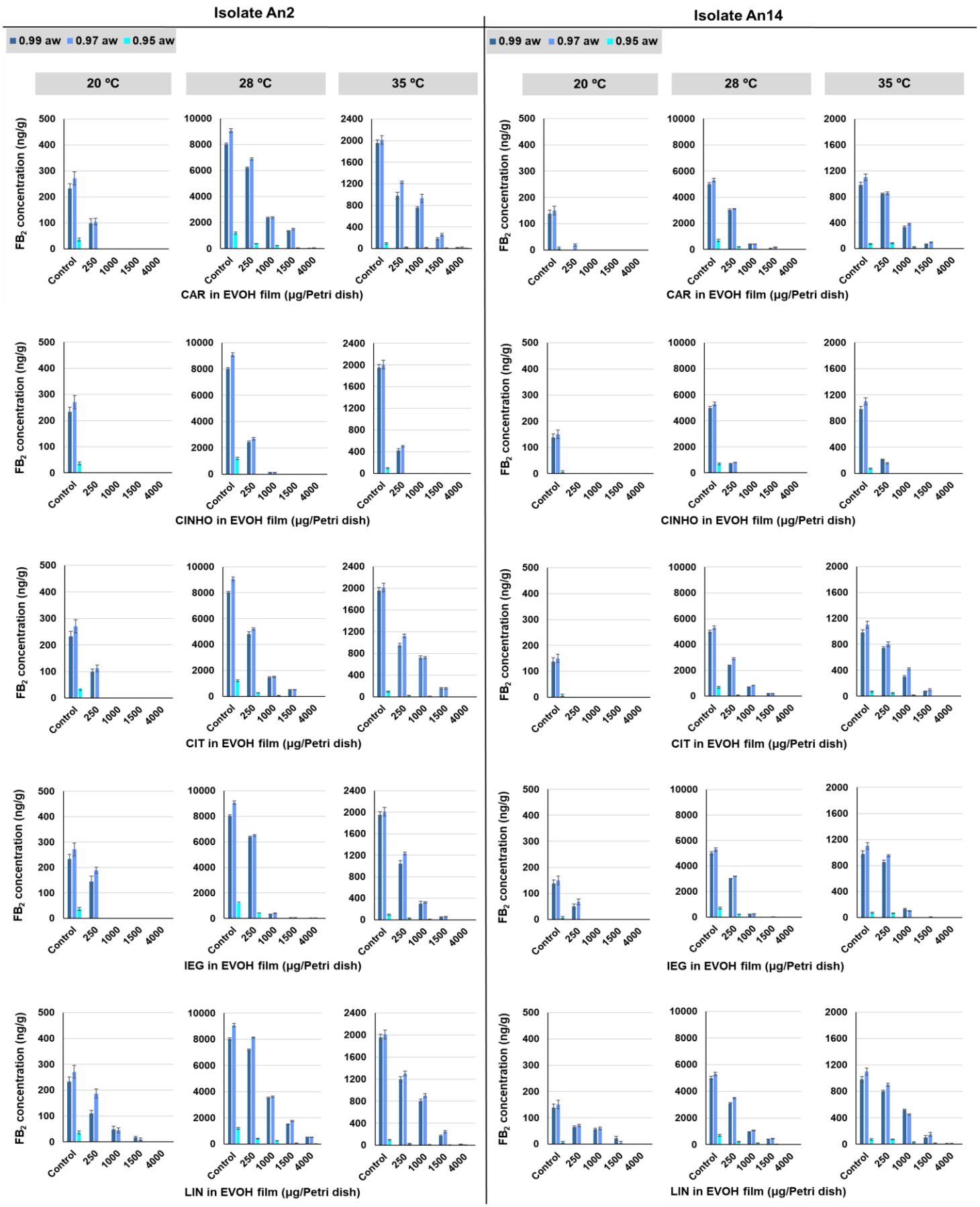

Figure 5

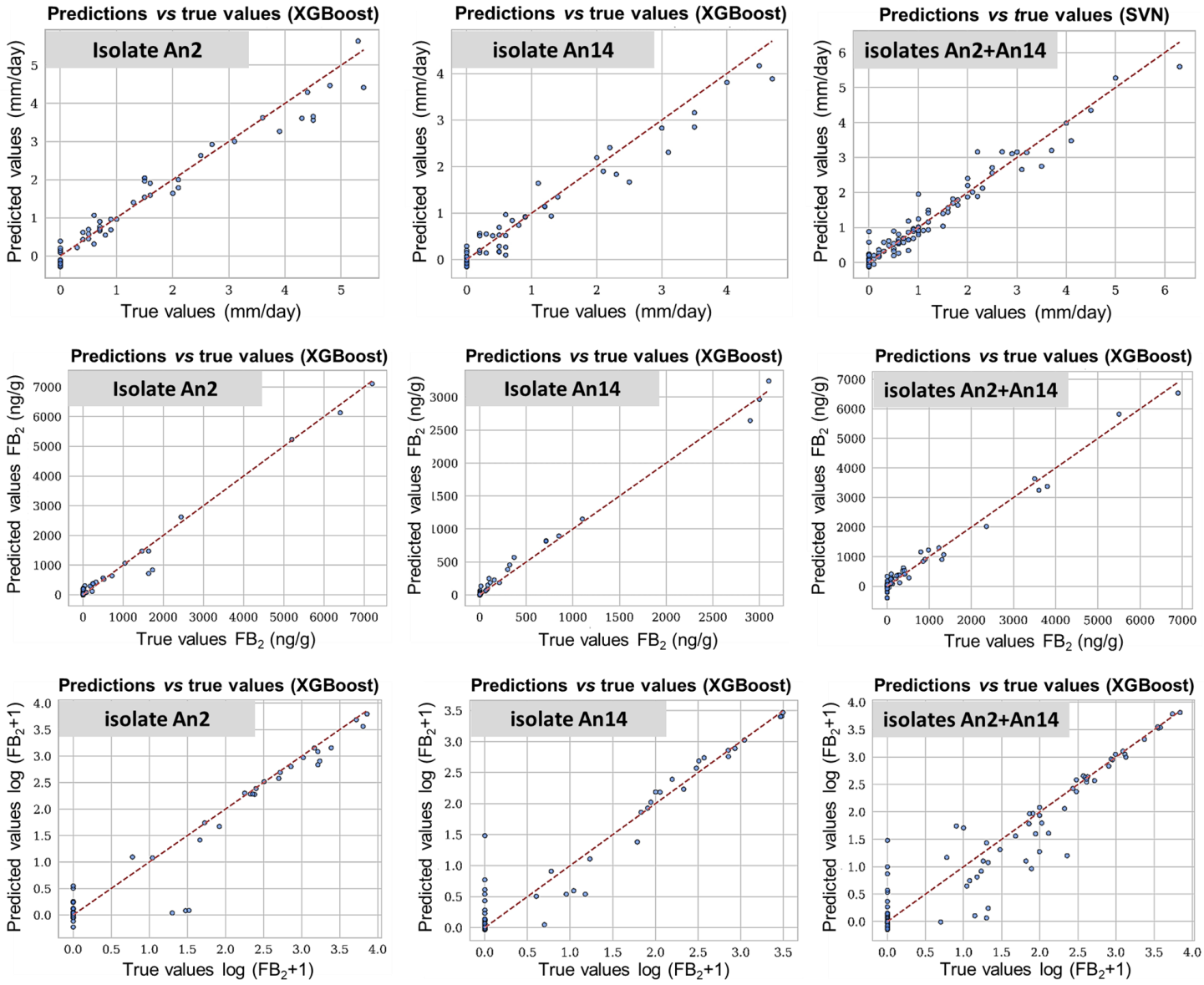

Declaration of competing interest

The authors declare that they have no known competing financial interests or personal relationships that could have appeared to influence the work reported in this paper.